Univerzita Karlova

3. lékařská fakulta

Dizertační práce

Improving the diagnosis of first-episode schizophrenia from magnetic resonance imaging using machine learning

Využití strojového učení v analýze dat z magnetické rezonance za účelem zlepšení diagnostiky časné schizofrenie

MUDr. Pavol Mikoláš

Školitel: Prof. MUDr. Tomáš Hájek, Ph.D.

Konzultant: MUDr. Filip Španiel, Ph.D.

Praha, 2018

Prohlášení:

Prohlašuji, že jsem závěrečnou práci zpracoval samostatně a že jsem řádně uvedl a citoval všechny použité prameny a literaturu. Současně prohlašuji, že práce nebyla využita k získání jiného nebo stejného titulu.

Souhlasím s trvalým uložením elektronické verze mé práce v databázi systému meziuniverzitního projektu Theses.cz za účelem soustavné kontroly podobnosti kvalifikačních prací.

V Praze, 1.6.2018

MUDr. Pavol Mikoláš Podpis

Poznámka k elektronické verzi:

Prohlašuji, že odevzdaná tištěná verze práce a verze elektronická nahraná do Studijního informačního systému (SIS 3.LF UK) jsou totožné. V elektronické verzi dizertační práce jsou zapracovány připomínky typografického typu. Tyto změny jsou přesně popsány v dodatku.

V Praze, 29.10.2018

MUDr. Pavol Mikoláš

Identifikační záznam:

MIKOLÁŠ, Pavol. *Využití strojového učení v analýze dat z magnetické rezonance za účelem zlepšení diagnostiky časné schizofrenie. [Improving the diagnosis of first-episode schizophrenia from magnetic resonance imaging using machine learning]*. Praha, 2018. 77s. Dizertační práce. Univerzita Karlova, 3. lékařská fakulta, Klinika psychiatrie a lékařské psychologie 3. LF UK, 2018. Školitel: Prof. MUDr. Tomáš Hájek.

Keywords: machine learning, support vector machine, resting state, functional connectivity, salience network, fMRI, fractional anisotropy, first episode schizophrenia spectrum

Klíčová slova: strojové učení, support vector machine, klidový stav, funkční konektivita, síť salience network, fMRI, frakční anisotropie, první epizoda schizofrenie

Acknowledgements

I am grateful to my supervisor Prof. Tomáš Hájek, who not only provided his cutting-edge scientific know-how in neuroimaging and machine learning, but also devoted a considerable portion of his free time to supervise my work. I especially appreciated his ethical and methodological rigorosity, as well as his ability to extract the essence into brisk, compelling formulations. It has been a pleasure to learn from him. I would like to thank my co-supervisor MUDr. Filip Španiel for designing and leading the amazing Early stage schizophrenia outcome (ESO) study, which gave rise to our findings. My work would not be possible without his enthusiastic support. I would also like to thank all the colleagues who contributed to my publications: Jaroslav Hlinka, Eduard Bakstein, Antonín Škoch and Zbyněk Pitra for providing their computational skills, Martin Matějka, Andrea Slováková and Tomáš Melicher for recruiting the patients, Prof. Thomas Frodl for reviewing the manuscripts critically, Leonardo Tozzi for his advice by visualizing the results. Finally, I am especially grateful to my wife Vendula Mikolášová, who supported me and provided me with enthusiasm.

Content

Abstract

Background: Early diagnosis of schizophrenia could improve the outcomes and limit the negative effects of untreated illness. Although participants with schizophrenia show structural/functional alterations on the group level, these findings have a limited diagnostic utility. Novel methods of MRI analyses, such as machine learning (ML), may help bring neuroimaging from bench to the bedside. Here, we used ML to differentiate participants with a first episode of schizophrenia-spectrum disorder (FES) from healthy controls (HC) based on neuroimaging data and compared the diagnostic utility of such approach with the utility of between group comparisons using classical statistical methods.

Method: Firstly, we performed a classical fMRI experiment in FES using a self/other-agency task (SA/OA) and compared FES (N=35) versus controls (N=35) using conventional statistics. We than classified FES and healthy controls (HC) using linear kernel support vector machine (SVM) from the resting-state functional connectivity (rsFC) and fractional anisotropy (FA) in 63/63 and 77/77 age- and sex-matched FES and HC participants. We also investigated the between-group differences in rsFC and FA using classical between-group comparisons.

Results: FES group exhibited a decreased activation during the emergent SA experience within the central medial structures (CMS), which reflects a biological correlate of FES. The SVM applied to the rsFC and FA distinguished the FES from the control participants with an accuracy of 73.0% (p=0.001) and 62.3 % (p=0.005), respectively. In the case of rsFC, the classification was significant when the anterior insula/salience network was used. The classification accuracy was not significantly affected by medication dose or by the presence of psychotic symptoms. The between-group differences in rsFC and FA overlapped with the regions contributing to the SVM classification.

Conclusions: Unlike classical between-group comparisons, ML in combination with rsFC and FA can be utilised for diagnostic classification, even early in the course of schizophrenia. The classification was likely based on trait rather than state markers, as symptoms or medications were not significantly associated with classification accuracy. Our results also support the role of anterior insula/salience network and CMS in the pathophysiology of FES.

Abstrakt

Úvod: Včasná diagnóza schizofrenie může omezit negativní dopad neléčené nemoci. Progresivní funkční a strukturální změny byly opakovaně detekovány metodami skupinové statistiky, avšak kvůli nízké senzitivitě a specificitě nenašly v klinické praxi dosud využití. Nové metody analýzy, jako například strojové učení, mají v kombinaci s neurozobrazovacími metodami v psychiatrii diagnostický potenciál. Provedli jsme klasifikaci pacientů s první epizodou schizofrenie a zdravých dobrovolníků založenou na neurozobrazovacích datech a srovnali možnosti jejího klinického využití s přístupy klasické skupinové statistiky.

Metody: V prvním kroku jsme provedli analýzu klasického fMRI experimentu v blokovém designu s využitím ‘‘self-agency‘‘ paradigmatu (SA) pomocí klasické skupinové statistiky. Následně jsme klasifikovali pacienty s FES a zdravé dobrovolníky pomocí linear support vector machine (SVM) z dat klidové funkční konektivity (rsFC) a frakční anizotropie (FA) pomocí strojového učení na souborech 63/63 (rsFC) a 77/77 (FA) pacientů/zdravých dobrovolníků, kteří byli jednotlivě matchováni podle věku a pohlaví.

Výsledky: U FES jsme detekovali nižší aktivaci během SA prožitku v centrálních mediálních strukturách (CMS). SVM byl schopen rozlišit pacienty od zdravých dobrovolníků s přesností 73.0% (p=0.001) (rsFC) a 62.34 % (p=0.005) (DTI). V případě rsFC byla přesnost klasifikace statisticky významná, když jsme použili konektivitu přední insuly/salience network. Výsledky analýzy pro obě modality nebyly ovlivněny medikací ani mírou symptomů. Meziskupinové rozdíly v rsFC a FA se překrývaly s oblastmi které nejvíc přispívaly ke klasifikaci pomocí SVM.

Závěry: Na rozdíl od přístupu klasického meziskupinového srovnání dokáže strojové učení s využitím klidové funkční konektivity a DTI rozlišit pacienty s FES od zdravých dobrovolníků na individuální úrovni. Klasifikace reflektuje spíše ‘’trait’’ nežli ‘’state’’ markry onemocnění, protože nebyla ovlivněna symptomy ani medikací. Výsledky na meziskupinové úrovni poukazují na význam přední inzuly/salience network a CMS v patofyziologii FES.

1. Introduction

Schizophrenia is often a life-long condition with an early onset and recurrent or chronic course (Andreasen et al., 2011; Rabinowitz et al., 2007). Despite its low prevalence (lifetime prevalence 4:1000, point prevalence 2.6-6.7:1000) it causes major health, social and economic burden (Chaiyakunapruk et al., 2016). As the onset of illness starts typically in the beginning of the productive age (20-30 years), many individuals with schizophrenia spend most of their lives in partial or total disability. It has been estimated, that schizophrenia accounts for 1.1% of the total disability-adjusted life years (DALY) and 2.8% of years lived with disability (Levav and Rutz, 2002) and is the eighth leading cause of DALYs worldwide in the 15–44 years age group. The economic burden of schizophrenia was estimated to range from 0.02% to 1.65% of the gross domestic product.

The clinical course of the disorder is associated with the progression of functional/structural alterations in the brain. In a subset of patients widespread progressive grey and white matter tissue reductions occur. These are positively correlated with the level of cognitive impairment (Andreasen et al., 2011). These alterations may not only complicate the treatment (Guo et al., 2013; Malla et al., 2011; Penttilä et al., 2010; Perkins et al., 2005), but are also associated with poor clinical and social outcome and may result in poor cognitive and social functioning. Therefore, the study of participants during their first episode of schizophrenia spectrum disorders is of high relevance, as it could improve early diagnosis. By limiting the effects of illness burden and medication exposure (Ho et al., 2011; Lieberman et al., 2001; Smieskova et al., 2009) this approach could also help identify biological signatures of the illness.

1.1. Diagnostics and clinical course of schizophrenia

The term schizophrenia was first used by the German psychiatrist Bleuler in 1908 to describe a disorder, or a group of disorders marked by characteristic splitting of psychic functioning in domains of thinking, perception, affect and social behavior (Fusar-Poli and Politi, 2008). Although the diagnostic criteria have evolved since that time, even now the diagnosis of schizophrenia is based on symptoms, rather than on the presence of a specific biomarker. Currently, the main symptoms include: thought echo, thought

broadcasting or insertion, delusions of controls, passivity or influence, hallucinatory voices or hallucinations in other modalities, persistent delusions, thought disturbance, neologisms, catatonic behavior, negative symptoms (apathy, emotional blunting, incongruence of emotional responses), significant changes in personal behavior, such as loss of interest, aimlessness and social withdrawal. Although the main diagnostic systems - ICD-10 and DSM-V have proved to be reliable in diagnosing the established disease, they tend to fail in the diagnostics of early stages, when the core symptoms might not be consistently present (Jablensky, 2010). Therefore, the search for biomarkers is crucial to improve not only the biological validity of the concept of schizophrenia, but also its clinical utility mainly in the early disease stages (Kendell and Jablensky, 2003).

1.2. Structural and functional connectivity in schizophrenia

In the last decades of neuroimaging research many neurobiological correlates of schizophrenia were identified. Abnormalities in functional and structural connectivity are present already at the level of the first-episode schizophrenia (FES), becoming more extensive in later stages of the disease (Canu et al., 2015; Mwansisya et al., 2017).

1.2.1 Functional connectivity in FES

Functional magnetic resonance imaging (fMRI) measures changes of oxygen-poor and oxygen rich blood in the brain (blood oxygen-level dependent signal - BOLD). These are the indirect markers of brain activity. Electrical activity of a group of neurons is a metabolically active process requiring oxygen and thus causing the concentration of oxygen-poor haemoglobin to increase. This results in vasodilatation and increased flow of oxygen-rich haemoglobin into the area with a time peak at 4-5 seconds (Malonek and Grinvald, 1996).

Initially, fMRI was used to map brain activation patterns during active tasks (e.g. a response to alternating sad or neutral faces). However, several authors also described spontaneous oscillations of BOLD signal at rest (Biswal et al., 1995; Ogawa et al., 1993). This observation gave rise to the discovery of resting state networks (RSNs) which are formed by regions of highly correlated BOLD activity (Biswal, 2012; Greicius et al., 2003). At least 9 such networks have been identified: the default mode

network (DMN), central executive network (CEN), salience network (SN), ventral and dorsal attention networks, visual network, motor/sensory network, basal ganglia module and cerebellum module (Bressler and Menon, 2010; Moussa et al., 2012). It is important to note, that although bearing "resting" in their name, the activity of RSNs can be also investigated during a particular task by measuring the correlation of signal between regions, rather than the actual activation.

The abnormalities in functional connectivity in FES were consistently detected especially in the fronto-temporal regions, such as the medial prefrontal cortex, dorsolateral prefrontal cortex (DLPFC) (Mwansisya et al., 2017). These two regions specifically are recruited within the DMN and CEN respectively. The DMN shows increased activation in internally focused tasks and a decreased activation in cognitively demanding states. In schizophrenia, reduced suppression of the DMN during various cognitive tasks represents a constant finding (Mwansisya et al., 2017). On the other hand, CEN is activated in externally oriented, cognitively demanding tasks. The tasks that activate DMN deactivate CEN, and vice versa. Moreover, the existing evidence supports a general role for the SN in switching between these two networks upon presentation of salient stimuli (Menon and Uddin, 2010; Nekovarova et al., 2014).

Functional brain imaging studies in healthy controls also confirmed that cortical midline structures (CMS), such as DMN are involved in the processing of self-specific stimuli that occurred across various functional domains (Murray et al., 2012; Northoff et al., 2006). The sense of agency (SA), i.e. the ability to distinguish actions and effects caused by oneself from events occurring in the external environment is a fundamental aspect of human cognition. A deficit in self-monitoring could underline both SA and the core psychotic symptoms (Fletcher and Frith, 2009). It has been proposed previously that aberrant activity in CMS regions of individuals with schizophrenia can lead to a misattribution of internally/externally generated stimuli (Farrer et al., 2004; Jardri et al., 2011). This can result in symptoms such as thought insertion and delusions of control. Anomalous self-related experiences precede frequently the onset of psychosis by many years (Schultze-Lutter, 2009). In addition, the self-monitoring deficit is detectable in unaffected siblings of patients with schizophrenia (Hommes et al., 2012) and it could represent a specific endophenotype within the schizophrenia spectrum. In

general there has been a considerable evidence that suggests a disturbance of the basic sense of self as a central feature of schizophrenia (Jeannerod, 2009).

In our study we employed a classical fMRI event-related study of the self-agency/other-agency (SA/OA) judgment (see Methods) in FES and in healthy controls to assess the differences in brain activation between the 2 groups during an emergent SA/OA experience (Spaniel et al., 2016). Using this fMRI paradigm we than explored the potential clinical utility of such classical between-group comparisons in psychiatric neuroimaging.

1.2.2 Structural connectivity in FES

Diffusion tensor imaging (DTI) is a unique technique that can map architecture of tissues in vivo. This is achieved by mapping the diffusion processes of water molecules in brain tissue using magnetic gradient field. An environment in which the water molecules can diffuse freely in all directions is called isotropic. In the brain, the diffusion is restricted by obstacles imposed by microstructure such as cell membranes, myelin sheaths and the microtubules. In such a case the environment is characterized by a certain degree of anisotropy (Jones et al., 2013). Thus, the DTI can be used to describe the properties of tissue microstructure, such as the organisation and density of white matter tracts, degree of myelination, crossing of fibres or membrane permeability.

Fractional anisotropy (FA) is a widely used scalar DTI-derived measure of diffusivity, which has gained popularity in clinical applications, such as differential diagnostic of stroke (Allen et al., 2012; Dong et al., 2004; Doughty et al., 2016). In psychiatry, abnormalities in fractional anisotropy on between-group level were detected across a variety of disorders, including FES.

According to Canu et al., (2015) were decreased FA values in FES detected predominantly in the corticospinal tract, long association white-matter fibers, interhemispheric connections cerebello-thalamo-cortical circuit and limbic system. Some studies also showed increased FA in the corticospinal tract and long association white-matter fibers.

Some research papers suggested that the alterations of microstructural properties are rather diffuse and present in the major white matter tracts rather than localized (Samartzis et al., 2014; Yao et al., 2013). This finding was so also reported by our study, where we showed, that the extent of FA reductions in patients increased with the sample size (Melicher et al., 2015). This was also confirmed in the recent ENIGMA study which included 4322 individuals (Kelly et al., 2017). Therefore the previously reported localized FA differences may be rather due to underpowered sample sizes.

1.3. Machine learning

In spite of the vast amount of neuroimaging discoveries achieved over several decades the diagnostic promise of neuroimaging in psychiatry has not yet been fully realised. One of the reasons is the low sensitivity/specificity of brain imaging findings. A large number of studies has shown statistical differences between patients with psychiatric disorders and healthy individuals. Yet, this has been primarily achieved by comparing groups of individuals using between group statistical comparisons, aiming at identifying differences at a minimum significance of $p<0.05$ (Milham et al., 2017). As The figure 1 illustrates, although being statistically significant, the typical between-group differences are based on relatively heterogenous populations, where the individual characteristics of patients and healthy persons largely overlap. Estimated effect sizes for a clinically relevant biomarker can range between a Cohen's d of 1.5-3.0, which the classical neuroimaging studies rarely achieve (Castellanos et al., 2013). Although the results of these predominantly univariate methods have contributed to our understanding of the mechanisms of psychiatric disorders, unfortunately they have not been suitable for use in clinical setting, where the focus is on the individual. To overcome this limitation of conventional statistical methods of analysis we need to extract significant information on the individual level and thus be able to make precise individualized predictions regarding the diagnosis, treatment and clinical outcome. This cannot be done using traditional statistical methods, but can be achieved using analytical tools from the field of machine learning/pattern recognition.

According to Dwyer et al., (2018) machine learning can be defined as a computational strategy that automatically learns methods and parameters to reach an optimal solution

to a problem rather than being programmed by a human *á priori* to deliver a fixed solution. An important characteristic of ML methods is that they improve their performance with training. One fundamental division of ML methods is into 'supervised' and 'unsupervised' methods. Supervised ML methods model the relationship between a set of predictors, or *features* and an outcome (Pereira et al., 2009). The outcome can be categorical (e.g. a classification of patients and controls) or continuous (a regression problem, e.g. prediction of age from structural brain scans (Hajek et al., 2017; Kolenic et al., 2018; Schnack et al., 2016). On the other hand the unsupervised ML is used where there is no specific outcome to be predicted. In such a case the algorithm is designed to detect an unknown structure in the data (e.g. unknown subpopulations of patients sharing specific clinical characteristics (Brodersen et al., 2014). An important subcategory of ML methods is the so called semi-supervised learning, which may be used in situations where the outcome (e.g. label) is known only for a small amount of data.

In this work we have attempted to apply the ML methods to the problem of clinical diagnosis in psychiatry. As this is a classification problem (we distinguished between two labels - patients and controls), we used exclusively the supervised ML. In this case two, ideally independent, datasets are necessary. The fist dataset is used as the 'training set'. The algorithm 'sees' the labels and extracts a predictive model from the features of the data. In a typical neuroimaging setting the features might be the individual voxels, volume or connectivity between different regions of interest. The classification itself is then performed on the second dataset - the 'test set'. Here the labels are unknown to the algorithm. The algorithm is able to estimate the correct labels when the prediction accuracy is significantly greater than chance (i.e. bigger than 50 %). The classification performance is measured by the classification accuracy, i.e. the amount of correctly classified subjects ((true positives + true negatives) / total number of subjects). Other typical measures are the sensitivity and specificity.

In order to extract the most possible information from the data during the learning phase, most researchers use the so-called *K*-fold cross validation scheme (CV). The original sample is divided in 2 subsamples (train and test) *K* times, so that each time 1/*K* subjects are left out as the ‘test’ set while the rest of the subjects (*K*-1/*K*) are used as the training set. This is repeated in *K* iterations. The resulting accuracy is the

average of the accuracies on individual runs. An example of a 5-fold crossvalidation is provided in figure 2. A common variant is the so called leave-one-out classification, where exactly 1 subject ist left out as the 'test' set on each run. The classification is than repeated until each subject was left out exactly once.

Many different machine learning algorithms exist (e.g. random forrest, naive Bayes, support vector machines, artificial neural networks etc. - for a more detailed overview and summary of their advantages and disadvantages in neuroimaging data analysis we recommend Iniesta et al., (2016). Their use in neuroimaging introduced a fundamental change in the data analysis with clinical intentions. Unlike conventional univariate statistical methods, which yield significant results on a group-level, multivariate machine learning classifiers are sensitive enough to accurately classify individual subjects (Haller et al., 2014). Where the conventional statistic uses inference about the known, well characterized datasets, machine learning learns patterns from the data and tries to generalise these in order to perform predictions about unknown data. These unique features of ML may help bring neuroimaging from the bench to the bedside (Hajek et al., 2015).

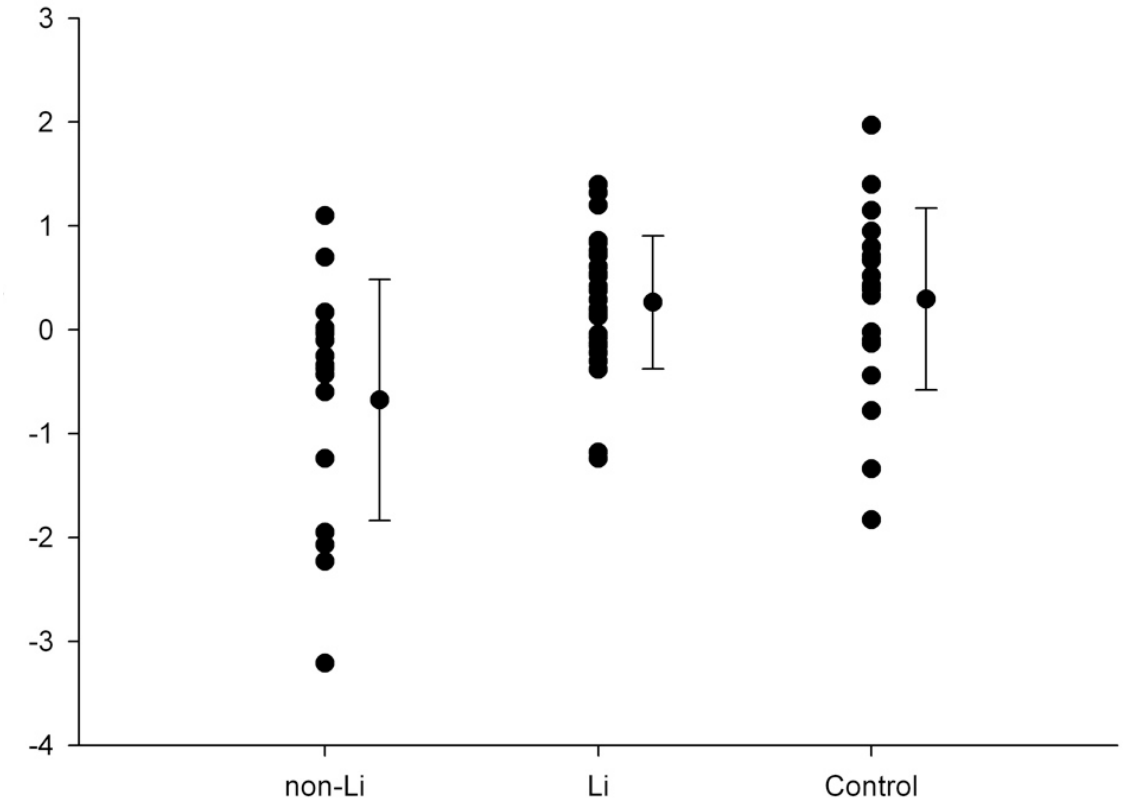

Figure 1. Distribution of the N-acetylaspartate findings in a typical neuroimaging experiment. The Z-scores reflect the N-acetylaspartate signal in the brain between 3 groups of subjects (patients not treated with lithium, patients on lithium and healthy controls). The findings in all groups are highly variable and they overlap to a great extent. In fact, a subgroup of patients (patients taking lithium) completely overlaps with the healthy controls. Although the differences between non-Li and other groups are statistically significant, they show low sensitivity and specificity and are of low clinical utility. Adapted according to Hajek et al., (2012). Li/non-Li - patients on/without lithium treatment, vertical axis - Z-scores of N-acetylaspartate signal in the brain measured using MRI spectroscopy.

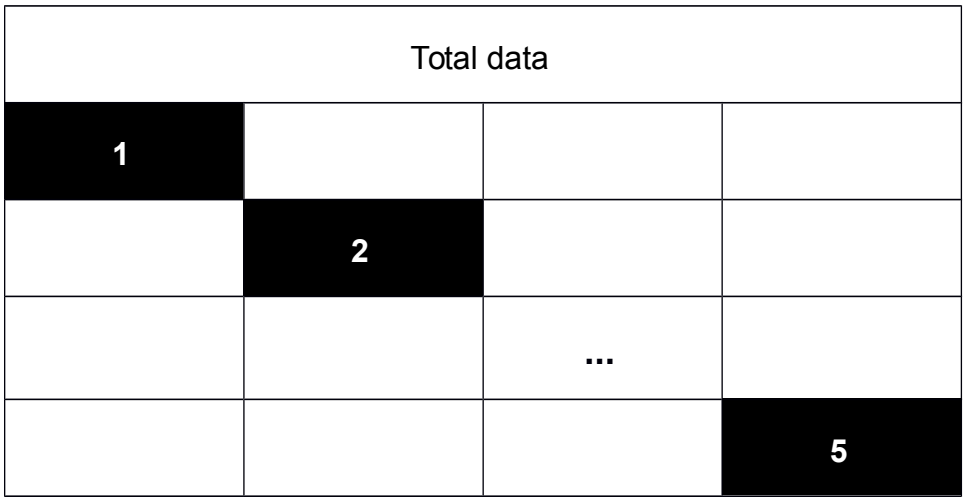

Figure 2. An example of a 5-fold cross-validation. On each fold, the data is split randomly in learning set (white) and test set (black). The procedure is repeated 5 times. Figure adopted from Iniesta et al., (2016)

1.4. Machine learning classification studies in FES

Brain imaging applications of machine learning in schizophrenia have mostly used gray-matter structural or functional MRI data. Most of them were performed in patients with the established disease rather than the first episode. Previous studies in FES have utilised structural MRI (Kasparek et al., 2011; Mourao-Miranda et al., 2012; Peruzzo et al., 2014; Zanetti et al., 2013), or task-based fMRI (Pettersson-Yeo et al., 2013), achieving classification accuracies from 54% to 90% using sample sizes ranging from 28/28 to 100/91 (FES/HC). Machine learning applied to resting state functional magnetic resonance imaging (rsfMRI) was used in several studies to classify patients with an established schizophrenia with accuracies between 65% and 95% using sample sizes from 8/10 to 69/62 (schizofrenia/HC) (Kambeitz et al., 2015), but not in FES. Similarly, other modalities, such as whole brain DTI have not yet gained comparable attention. Previous machine learning studies that utilized DTI for the classification of FES and control participants reported classification accuracies between 65.79% and 76.1%, unfortunately with very low sample sizes of 19/19 and 23/23 (FES/HC) (Pettersson-Yeo et al., 2013; Zanetti et al., 2013). As ML benefits from larger sample-sizes, larger studies are needed to investigate the diagnostic potential of DTI in early stages of schizophrenia (Schnack et al., 2014). Due to the clinical relevance for making early diagnosis and limited effects of illness burden and medication exposure it is particularly necessary to focus on the early disease stages, such as FES. Driven by the lack of data (rsFC) or their insufficiency (DTI) in FES we decided to focus on the analyses of these two modalities.

1.5. Objectives

In this study we firstly performed a task-fMRI experiment using the SA/OA judgement paradigm in patients with FES (Spaniel et al., 2016). We interpreted the data in terms of classical between-group comparison and illustrated the disadvantages of such approach regarding its potential clinical utility. Secondly, to the best of our knowledge, we performed the first study using resting-state functional connectivity to differentiate participants with FES from healthy controls using machine learning (Mikolas et al., 2016). Thirdly, we investigated whether machine learning applied to brain DTI data will differentiate between 77 FES and 77 control participants, which was the largest ML/DTI

study in FES available at the time (Mikolas et al., 2018). Finally, to illustrate the low specificity and sensitivity of classical between group statistics, we also compared the results obtained by machine learning with those derived from traditional between-group analyses using the same modalities (rsFC and DTI).

2. Methods

2.1. Study design

We recruited participants through the Early-Stage Schizophrenia Outcome study (ESO), a prospective trial of first-episode schizophrenia spectrum subjects, conducted in Prague and the Central Bohemia areas (Melicher et al., 2015). The study was carried out in accordance with the latest version of the Declaration of Helsinki. A written informed consent was obtained from all of the subjects and the local ethics committee approved the protocol.

2.2. Subjects

To ensure generalizability we recruited patients during their first hospitalization in the Psychiatric Hospital Prague, which is a general psychiatry hospital (1200 beds) with a catchment area of over 1.5 million subjects. Briefly, we recruited patients with FES, who: 1) were undergoing their first psychiatric hospitalization, 2) had the diagnosis of schizophrenia or acute and transient psychotic disorders as made by a psychiatrist according to the ICD-10 criteria, 3) had less than 24 months of untreated psychosis. Patients with psychotic mood disorders, including schizoaffective disorder, bipolar disorder and unipolar depression with psychotic symptoms, were excluded from the study. We rated the symptom severity at the time of scanning using the Positive and Negative Syndrome Scale (PANSS) (Kay et al., 1987). All of the patients were treated with antipsychotic drugs at the time of the MRI scanning. The MRI scanning was performed during the first hospitalization, as soon as the patients were able to understand the purpose of the study and undergo the fMRI protocol.

We were primarily interested in subjects at the early stages of illness, as this is one of the few ways, how to limit the effects of previous psychotic episodes and how to minimize exposure to medications or comorbid conditions. This approach minimizes the effects of confounding variables, which could alter classification accuracy. Consequently, as many of the participants were hospitalized shortly after developing

symptoms, some of them did not meet the duration criteria for schizophrenia at the time of scanning. These patients received the working diagnosis of acute polymorphic psychotic disorder which is congruent with DSM-IV defined brief psychotic disorder.

2.3. Healthy controls

The healthy control subjects (HC) were recruited via an advertisement from a similar sociodemographic background and were matched to FES participants by age and sex on an individual basis. The main exclusion criteria for the control subjects were a personal lifetime history of any psychiatric disorder, or any substance abuse, established by the Mini International Neuropsychiatric Interview (M.I.N.I.) (Lecrubier et al., 1997). We also excluded any family history of a psychiatric illness in first or second degree relatives.

Further exclusion criteria, for both the patients and the healthy controls included current neurological disorders, a lifetime history of seizures, or a head injury with altered consciousness, an intracranial haemorrhage, a history of mental retardation, substance dependence, and any contraindications for MRI scanning.

2.4. fMRI data acquisition

The data was acquired in the Institute of Clinical and Experimental Medicine in Prague by a 3T Siemens Trio MRI scanner (Siemens, Erlangen, Germany) equipped with a standard head coil. For the fMRI data pre-processing, the subjects were scanned using a structural T1-weighted (T1W) 3D-MPRAGE sequence (repetition time (TR) 2 300 ms, echo time (TE) 4.63 ms, bandwidth 130 Hz/pixel, field of view (FOV) 256x256 mm, matrix 256 x 256, 160-224 contiguous sagittal slices, a voxel size of 1x1x1mm, GRAPPA, and Acceleration Factor 2). Functional images sensitive to the BOLD contrast were measured with a gradient echo echo-planar sequence (GRE-EPI, TR=2000 ms, TE=30 ms, flip angle 90°, bandwidth 2 232 Hz/pixel, without parallel acceleration). The rsFC scans were acquired with FOV= 192 mm×144 mm, matrix size 64x48, a voxel size of 3x3x3 mm, each volume with 35 axial slices without an inter-slice gap, and a total of 400 volumes. The task-fMRI scans were acquired with FOV =

192 mm × 192 mm, matrix size 64 × 64, each volume with 30 axial slices without an inter-slice gap, a total of 240 volumes).

2.5 Task fMRI SA/OA agency paradigm

During the task-fMRI experiment, the SA experience was elicited and contrasted against the OA perception in a motor task using manipulation of the degree of incongruence between the subject's motor intentions and the visual feedback, which is a widely used approach in the research of self-related processing (Sperduti et al., 2011). A simple scene (figure 3) was presented using Java based software running on a computer connected to an LCD projector. Stimuli were projected onto a mirror attached to the head coil through a screen positioned at the head end of the scanner bore. Participants were instructed to maintain steady movements of a cursor using a MRI-compatible joystick. They were told that occasionally they would not see their own movements, but instead they would observe cursor movement intrusions that looked like they were driven by the experimenter from outside of the scanner. In reality, software-based random angular distortions of subject's own actions were generated throughout OA blocks. This approach was necessitated due to differences in agency processing in human-human interaction compared to human-computer co-acting (Obhi and Hall, 2011). Using this approach we were able to manipulate the sense of agency at the onset of the corresponding SA/OA block. During the OA block the angular cursor movement was influenced by the software constantly. However, the speed of cursor movement was dependent only on the velocity of joystick movements driven by examined subjects in both blocks (ie, OA and SA, see further below). Angular distortion in OA blocks were added to actual angle in polar coordinate system in a fixed manner depicted in figure 4. Despite usage of this fixed pattern of distortion, debriefing revealed no evidence for recognition of either exact regularity or artificiality of this approach. As intended, all participants attributed cursor movement deviations during OA to the other human subject. The design alternated between 12 OA and 12 SA blocks with an absence of any visual-feedback distortion. Each block lasted 20 seconds. Participants were blinded to the sequentially and length of both SA and OA blocks. The blocks were presented in fixed alternating sequence. Post-experimental debriefing revealed no impact of this regular design on genuine experience of SA or OA. Experimental subjects were instructed to keep moving the cursor either inside the central square if the movement they saw was subjectively interpreted as

influenced by the "experimenter," or shift it promptly to the outer corridor as soon as they gained a distinct feeling of SA. In such a case they were instructed to remain moving in this sector until the subjective onset of the next "experimenter's" intrusion. No movement cessation was allowed during the task. To ensure that participants fully understood the task prior, all subjects underwent 3-minute training period in the scanner. Java-based software enabled us to record entire cursor track. This way we could confirm subsequently that all subjects enrolled in this study were compliant with the instructions. In addition, the software allowed for recording the exact coordinates of the cursor and thus track the cursor in real time. Therefore, target events (TEVS - i.e. when the cursor crossed the boundaries of the central square towards the outer corridor during a time-window encompassing the entire SA block) could be accurately determined. TEVS represented behavioral references to an emergent SA experience, which was the main interest of the study. Fixed OA onsets were initiated by software driven shift of the cursor into the central square at the predefined start of all OA blocks. In order to analyze BOLD correlates of an emergent SA/OA insight, we used 10-second episodes with onsets cued either by individual TEVS (further in the text as "SA condition"), or beginning of OA block (further in the text as "OA condition"). TEVS detection allowed us to minimize potentially impaired overall performance.

2.6. Task fMRI data processing

The task-related BOLD response was assessed using finite impulse response (FIR) with the length of 10 seconds in all participants (Henson et al., 2002). A general linear model was used to provide estimates of the signal changes at 6 time points shifted with an interval of 1 second since the onset of TEVS (having constant time window of 10 s), without making a priori assumptions about the shape of the hemodynamic response function. This approach enabled us to avoid errors associated with ill-fitting canonical models (Handwerker et al., 2004). The beta estimates for the FIR models entered a second level analysis (FWE corrected, $P < .05$). A time bin 5 seconds after TEVS was chosen as the peak BOLD response occurred during this period for both groups pooled together. Identical 5-second delay after fixed OA block onset was arbitrarily used for the OA condition as well.

Individual first-level contrast images were generated for the SA and OA conditions respectively (FEW corrected, $P < .05$). For the between-group analysis, 2-sample t test was performed at the whole brain level (FWE corrected voxel-wise, $P < .05$, minimal cluster size > 20 voxels). The anatomical localization was defined using the Talairach Daemon Atlas (Lancaster et al., 2000).

A post hoc SPM8 multivariate regression analysis was conducted to determine the effect of psychopathology (PANSS) and antipsychotic-dosages (CPZ) on functional activation, respectively. The analysis was confined to areas that demonstrated significant between-group activation differences (the medial frontal gyrus and the posterior cingulate gyrus).

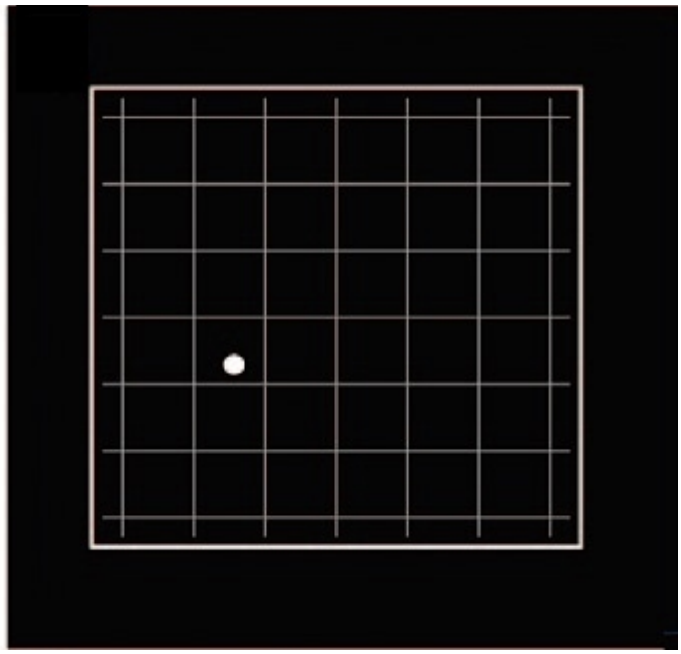

Figure 3. A representative screenshot of self/other-agency judgment task used in the functional magnetic resonance imaging (fMRI).

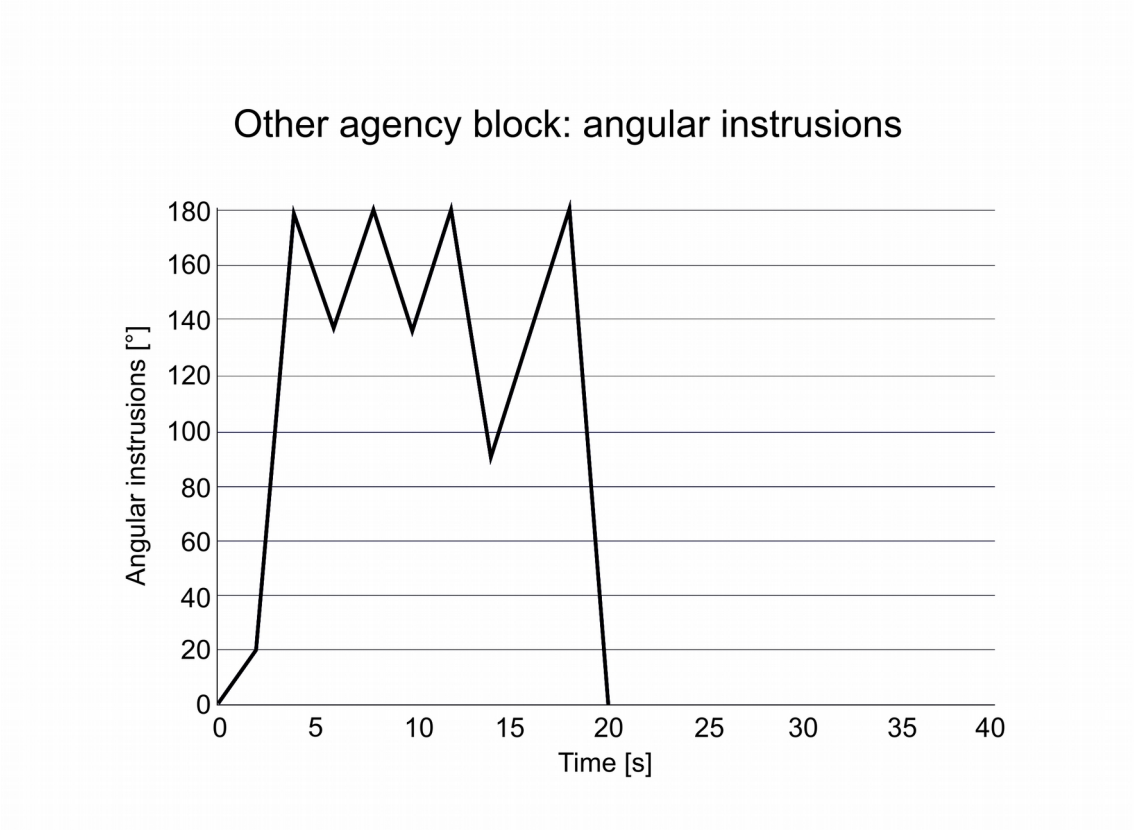

Figure 4. Angular intrusions introduced during other-agency (OA) block. We manipulated the sense of agency at the onset of the corresponding SA/OA blocks using software-based random angular distortions of subject's own actions.

2.7. Statistical analysis of behavioral measures within the task-fMRI

We evaluated the between-group comparisons in response accuracy during SA/OA judgment. This measure referred to the proportion of time spent in a proper segment of the visual scene during a corresponding block with and without distortion of visual feedback. In a second analysis we evaluated the difference in the number of TEVS initiating SA conditions that entered the final fMRI analysis. Whereas the first variable objectively reflected overall performance, the second measure served as a subjective indicator of the SA/OA experience in which BOLD signal changes were subsequently calculated. Between-group differences were analyzed by means of unpaired 2-tailed Student's t test, $P < .05$.

2.8. Resting-state functional connectivity data processing and analysis

Functional/structural data were pre-processed and analysed using tools implemented in the MATLAB 7.14 (R2012a) software. Slice-timing, realignment, regression of nuisance covariates (white matter and CSF signal, voxel specific head motion, mean signal), normalisation and smoothing of the functional images, as well as normalisation of the structural T1 images, were performed by an SPM8-Data Processing Based Toolbox Assistant for the Resting-fMRI (DPARSF) (Chao-Gan and Yu-Feng, 2010), and the Resting-State fMRI Data Analysis Toolkit (REST) (Song et al., 2011). The images were smoothed with an 8x8x8 Gaussian kernel. We applied temporal filtering over the frequency band of 0.008-0.09 Hz.

We calculated the resting state functional connectivity for all of the subjects between pre-selected ROIs and the voxels in the rest of the brain (seed based connectivity) using pre-processing pipelines which are well established and often used in the field i.e. (Alonso-Solís et al., 2012; Craddock et al., 2009; Venkataraman et al., 2012). We selected 3 ROIs, which correspond to the three networks of interest, i.e. posterior cingulate gyrus for the DMN, dorsolateral prefrontal cortex (DLPFC), as represented by the middle frontal gyrus for CEN and anterior insula (aINS) for the SN. The posterior cingulate gyrus and the DLPFC were selected from the AAL atlas (Tzourio-Mazoyer et al., 2002). This atlas does not provide parcellation of insula, which we obtained from Freesurfer (sulcus circular insulae) (Destrieux et al., 2010; Fischl et al., 2004; Menon

and Uddin, 2010; Palaniyappan et al., 2013; Sridharan et al., 2008). As patients with established SZ as well as those with FES show reduced asymmetry of resting state FC, we used ROIs from both sides as seeds in each model (Cabral et al., 2014; Damoiseaux et al., 2006; Guo et al., 2014; Swanson et al., 2011). Thus, for each subject, we calculated three connectivity maps, including connectivity between 1) bilateral anterior insula, 2) bilateral posterior cingulate, 3) bilateral middle frontal gyrus and the rest of the brain. Correlation coefficients were transformed into Z-scores by Fisher's transformation. These first level individual subject connectivity maps, were subjected to machine learning.

The second level functional connectivity analysis was performed by DPARSF (Chao-Gan and Yu-Feng, 2010). The differences in the seed-based FC between the patients and the controls were tested using a two sample t-test. The results were FWE corrected with a significance threshold $p<0.05$ on a cluster level. Only clusters exceeding 20 voxels were considered significant. In order to compare the uncorrected differences in the seed-based FC with the weight distribution obtained by the SVM, we performed a t-test on an uncorrected level, with a cluster level of $p=0.001$.

2.9. DTI data acquisition

The images were acquired on a 3T Siemens scanner in the Institute of clinical and experimental medicine in Prague, using a Spin-Echo EPI sequence with 2 acquisitions in 30 diffusion gradient directions, TR = 8300 ms, TE = 84 ms, $2 \times 2 \times 2$ mm^3 voxel size, b-value 900 s/mm^2 . DWI data were first visually inspected to check their quality. Subjects with excessive image distortion due to B0 inhomogeneity were excluded. Individual DWI volumes of each subject were inspected and when containing artifacts (k-space spikes, signal void due to movement) were excluded from further processing. If the number of volumes with artifacts per subject was greater than 11, the subject was excluded completely.

2.10. DTI data preprocessing

As described in our previous study (Melicher et al., 2015), we preprocessed the DWI data using FSL tools (Jenkinson et al., 2012). Movement and eddy current distortions

were corrected by affine registration using FLIRT. The mean dislocation estimated by FLIRT was checked and one subject with excessive value (6.4 mm) was replaced. Maximal value of mean dislocation per subject included in the study was 3.2 mm. The skullstrip was done by BET. The eigenvalues, eigenvectors and subsequent fractional anisotropy, axial and radial diffusivity were estimated by DTIFIT.

To foster compatibility with other studies, we chose an established method of FA preprocessing – the Tract Based Spatial Statistics (TBSS), implemented in the FMRIB's Software Library (FSL) (Amarreh et al., 2014; Damoiseaux et al., 2006; Haller et al., 2014, 2012; Pettersson-Yeo et al., 2013; Smith et al., 2004; Wu et al., 2016). We used the standard protocol, as described in the TBSS manual. All of the subjects' FA data were registered to a pre-defined target FMRIB58_FA using nonlinear registration FNIRT (Jenkinson and Smith, 2001). Next, we created a common skeleton representing all major white matter tracts. As it is necessary to maintain the train/test data separation in machine learning analyses, we did not use the study-specific skeleton option. Instead, we used the standard skeleton derived from the FMRIB58_FA template, as recommended by the manual. The white-matter skeleton was thresholded at recommended 0.2 FA threshold. Finally, all FA data were projected onto this skeleton. As a result, each subject was represented by a single 3D skeletonized FA image.

2.11. TBSS between groups comparisons

In order to indirectly compare the ability of SVM to make prediction about the individual subjects with the actual between-group differences in FA, we compared the skeletonized FA data between FES and HC. This was performed using the Randomise tool (Nichols and Holmes, 2002; Winkler et al., 2014), with the threshold free cluster enhancement (TFCE) for the family-wise error (FWE) correction at $p<0.05$ (Smith et al., 2006). The regions with significant differences in FA were labeled according to JHU ICBM-DTI-81 White Matter Labels and Tractography Atlas provided within the FSLView package.

2.12. Machine learning classification

We examined the diagnostic utility of the most standard and widely used ML paradigm, the support vector machines (SVM). Specifically, we applied a linear SVM implemented in the PRONTO toolbox v 2.0 (Schrouff et al., 2013). A linear SVM is suitable for analyzing high dimensional data such as whole-brain scans while keeping the computational pipeline relatively simple with low computational requirements (LaConte et al., 2005; Mourao-Miranda et al., 2012). This makes it superior for potential clinical setting over complex machine learning pipelines.

In the learning phase the SVM models the representation of cases as points in space and then constructs hyperplanes that separate the cases of different outcome labels. Individual data contribute to the calculation of the hyperplane with a specific weight vector (figure 5). The support vectors are the data which lie parallel to the hyperplane and if their position changes, consequently changes the position of the whole hyperplane. When there are more possibilities of constructing the hyperplane, the SVM chooses the hyperplane which distinguishes between the labels so that the gap between both groups (margin) is as wide as possible. On the other hand, in real case scenarios it is not possible to construct an ideal hyperplane and some subjects will be misclassified. The amount of mistakes can be penalized and this penalty can be optimized using the so-called C parameter (see below). In the classification phase the position of a new case relative to the hyperplane determines to which label it will be assigned (Iniesta et al., 2016).

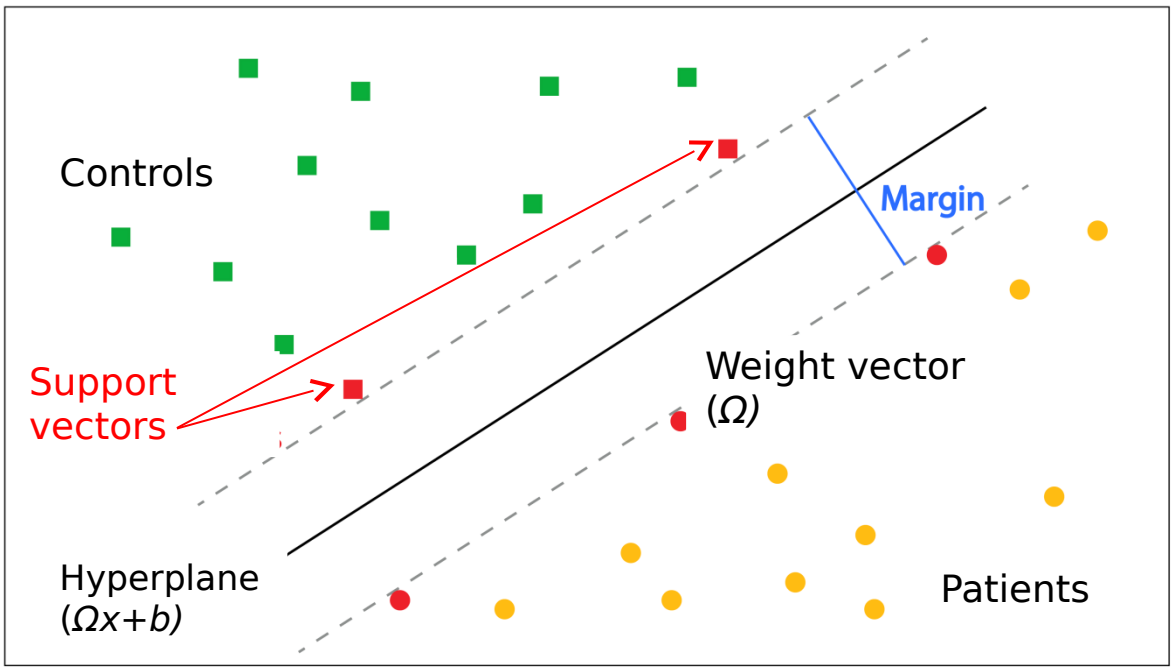

Figure 5. Illustration of the linear SVM. The SVM constructs a hyperplane which distinguishes between the labels so that the margin between both groups is as wide as possible. Individual data contribute to the calculation of the hyperplane with a specific weight vector (*Ω*). *b* - bias. Adapted according to http://www.coxdocs.org and Iniesta et al., (2016).

We utilized a linear kernel SVM, which is less prone to overfitting than non-linear SVMs. Linear kernel SVMs have a single parameter C, that controls the trade-off between having zero training errors and allowing misclassifications. Similar to other studies, we used the default parameter C=1 (Hajek et al., 2015; Mourao-Miranda et al., 2012; Rocha-Rego et al., 2014). The SVM performance for whole-brain classification does not change for a large range of C values and only degrades with very small C values (LaConte et al., 2005). Thus, modifying the C threshold was suggested only when the dimensionality of the data is smaller than the number of examples (e.g. classification based on small ROIs), which was not the case in our study. Others have suggested that using a sample-dependent optimization of the parameter C may improve the performance of the model (Franke et al., 2010; Nieuwenhuis et al., 2012). However, the aim of this study was not to optimize the SVM methods and attempting to optimize the parameter C would complicate clinical utility. Our goal was to reduce the methodological heterogeneity and use a simple, 'out of the box' approach, which could be applicable in clinical setting (Mourao-Miranda et al., 2012). Thus we used the default setting of C=1.

As the subjects were matched one-to-one according to age and sex, in order to retain this matching within the analysis, we performed a leave-one-subject-per-group cross-validation. Specifically, on each run, one subject from each group was assigned to the testing set and the remaining subjects were assigned to the training set. The classification was then performed on the two subjects in the test set. The resulting cross-validation procedure comprised 63 (rsFC) and 77 (FA) folds.

The classification accuracy was expressed as the total number of correctly classified test subjects divided by the total number of subjects. The statistical significance of the obtained classification accuracy was tested on 1,000 randomly permuted datasets, with a random assignment of the group to all subjects. A resulting null-hypothesis distribution was used to calculate the p-value of the accuracies, i.e. the proportion of the permutations that yielded a greater accuracy than the accuracy found for the classification models.

In case of the rsFC analysis, we applied the SVM to the individual subject functional connectivity maps. We estimated three separate SVM classification models (one for each of the three ROIs corresponding to the three pre-selected resting state networks). In order to remove zero voxels, all normalised brains were extracted using the BET tool implemented in the FSL package (Smith et al. 2004) and multiplied with each other in order to generate a common mask. The ML analyses were restricted to grey matter, by using a normalised grey matter mask provided by Dr Wager's lab (http://wagerlab.colorado.edu/wiki/doku.php/help/core/brain_masks). Each functional connectivity map comprised 52941 voxels (features).

For the DTI analysis, we applied the linear SVM to pre-processed skeletonized FA images from 77 FES patients and 77 controls. A common mask was applied to exclude voxels, which were not present in all subjects (Schrouff et al., 2013). The common mask contained 129154 voxels.

Both samples (rsFC and DTI) partially overlapped. 44 patients and 52 controls were present in both samples, i.e. 68% patients and 81% controls in the rsFC sample and 57% patients and 68% controls in the DTI sample.

2.13. Analysis of the effects of medication and symptoms

We attempted to clarify the contribution of medication and symptoms in several ways: 1) we compared symptoms and medication dose between correctly and incorrectly classified subjects using an independent sample T-test.; 2) We used a linear regression to assess the association between classification accuracy (value of the SVM decision function) and medication dose (expressed as chlorpromazine equivalents - CPZ) or symptoms, 3) we modeled the effects of covariates on functional connectivity using machine learning. Of note, in machine learning, removal of confounding covariates can violate the basic train/test assumption by introducing the information about the whole dataset before introducing labels. Therefore covarying for medication dose or symptoms would not be optimal. To counter this problem, we thus used another ML approach - Gaussian process regression (GPR) implemented in the PRONTO Toolbox v. 1.1 in the case of the rsFC data (Rasmussen and Williams, 2008) and the the kernel ridge regression (KR) implemented in PRONTO Toolbox v. 2.0 in the case of DTI data

(Schrouff et al., 2013; Shawe-Taylor and Cristianini, 2006). Both regression models utilize multivariate information to predict a continuous variable.

Using linear model in this case could easily lead to underfitting in case of non-linear relationship. Therefore, by harvesting as much of the confounding relationship as possible, the GPR and KR ensures that we exhaustively investigated and quantified the contribution of potential confounding factors to our findings. Specifically, we tested whether GPR or KR can estimate the chlorpromazine dose, or the total PANSS and 3 subscales (positive, negative, general), on the day of scanning from the the rsFC maps or the pre-processed FA skeletons. In the case of the rsFC, we only applied these analyses to SN which differentiated FES from controls above chance level.

2.14. Discriminating maps (SVM weight vector)

The use of linear kernel SVM allowed us to directly extract the weight vector as an image (the SVM discrimination map). The SVM decision hyperplane is described by a weight vector and an offset. The weight vector is orthogonal to the hyperplane and corresponds to the most discriminating direction between the groups. Every voxel contributes with a certain weight to the decision boundary or classification function. The SVM weight vector is a linear combination or weighted average of the support vectors and is the spatial representation of the decision boundary. We plotted this weight map as a brain image to show the relative importance of the voxels in discriminating the classes.

3. Results

3.1. Self-agency task-fMRI

3.1.1. Demographic data

We performed the analysis of the SA/OA Task-fMRI on the sample of 35 FES patients and 35 age-matched healthy controls without a personal or a family history of psychiatric disorder. For a detailed description of the samples please see table 1.

3.1.2. Behavioral performance

HC showed significantly higher overall response accuracy compared to FES (HC: mean 84.6, SD 5.9, FES: mean 65.9, SD 16.8; t = 2.83, P = 0.006). There was no statistically significant correlation between the PANSS (positive, negative, general psychopathology and total) score and overall response accuracy. There was a similar number of TEVS in FES (mean 11.9, SD 0.2) and HC (mean 12.0, SD 0.2; $t = 0.58$, $P = 0.6$).

3.1.3. Between-group differences

During the SA condition, HC showed greater activation than FES in 2 significant clusters (table 2, figure 6) located in the anterior portion of the CMS within the left medial frontal gyrus (BA 10) and the posterior part in the posterior cingulate gyrus (BA 31), respectively (FEW corrected, voxel-level, $p < .05$). There were no regions in which FES showed greater activation than HC. During the OA condition, there were no differences in activation/deactivation between the groups during OA experience.

To illustrate the heterogeneity of individual differences within the statistically significant clusters we plotted the average beta values in scatter plot graphs in figure 7.

3.1.4. Relationship of PANSS and medication to fMRI activity

There were no associations between the task-related activation and potential confounds (antipsychotic dose expressed as chlorpromazine equivalent or PANSS positive, negative, general psychopathology and total scores) within ROI consisting of CMS (FWE corrected, $P < .05$).

	Controls (n=35)	**Patients (n=35)**	**Note**
Sex – female N (%)	21 (61.2%)	17 (48%)	p=0.34
Age, mean (S.D.)	30.6 (9.2)	29.4 (6.7)	p=0.56
Median duration of illness, weeks (SD)	n/a	19.6 (16.6)	n/a
Drug dose upon MRI – median chlorpromazine equivalent (SD)	n/a	412 (186.5)	n/a
PANSS positive mean (SD)	n/a	17.6 (7.5)	n/a
PANSS negative mean (SD)	n/a	16.4 (4.8)	n/a
PANSS general mean (SD)	n/a	37.1 (10.4)	n/a
PANSS total mean (SD)	n/a	71.2 (19.0)	n/a

Table 1. Demographic and clinical data of the healthy controls and the patients (SA/OA Task-fMRI). S.D. – Standard Deviation; MRI – Magnetic Resonance Imaging; PANSS = Positive and Negative Syndrome Scale

Cluster size	t Value	Talairach Coordinates			Hemisphere	Region
		x	y	z		
168	5.4	-4	51	2	left	Medial frontal gyrus, BA 10
40	5.0	-8	-32	36	left	posterior cingulate gyrus, BA 31

Table 2. Results of between-group analysis for contrast between self-agency experience and other-agency. HC > FES. Whole brain analysis, FWE (Family-Wise Error) correction of *P* value ≤ .05 with a minimum cluster consisting of >20 voxels. BA, Brodmann area.

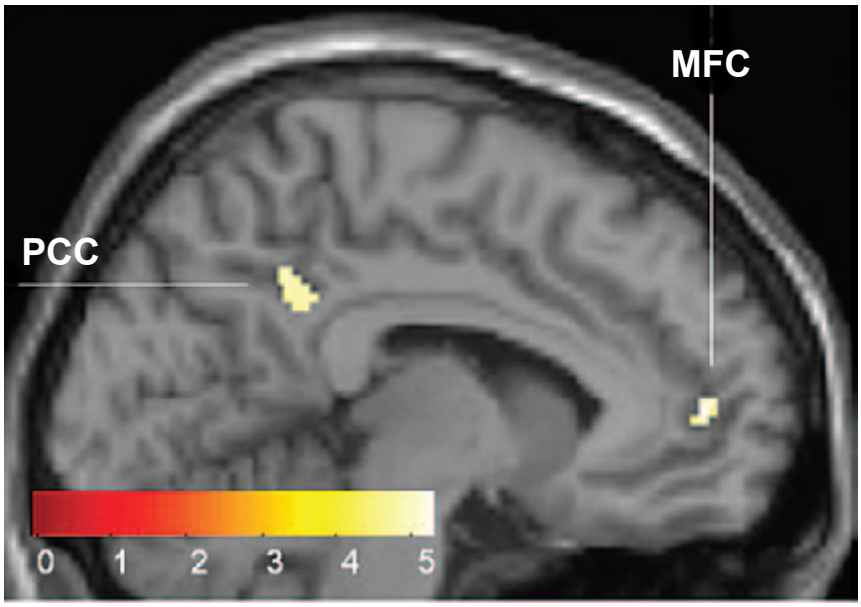

Figure 6. Whole-brain between-group analysis showing the regions that were significantly more active in the control group relative to the first-episode schizophrenia-spectrum (FES) group during self-agency judgment. Family-Wise Error (FWE) corrected, voxel level, $P < .05$. Color bar represents t values. MFC - mediofrontal cortex, PCC - posterior cingulate cortex.

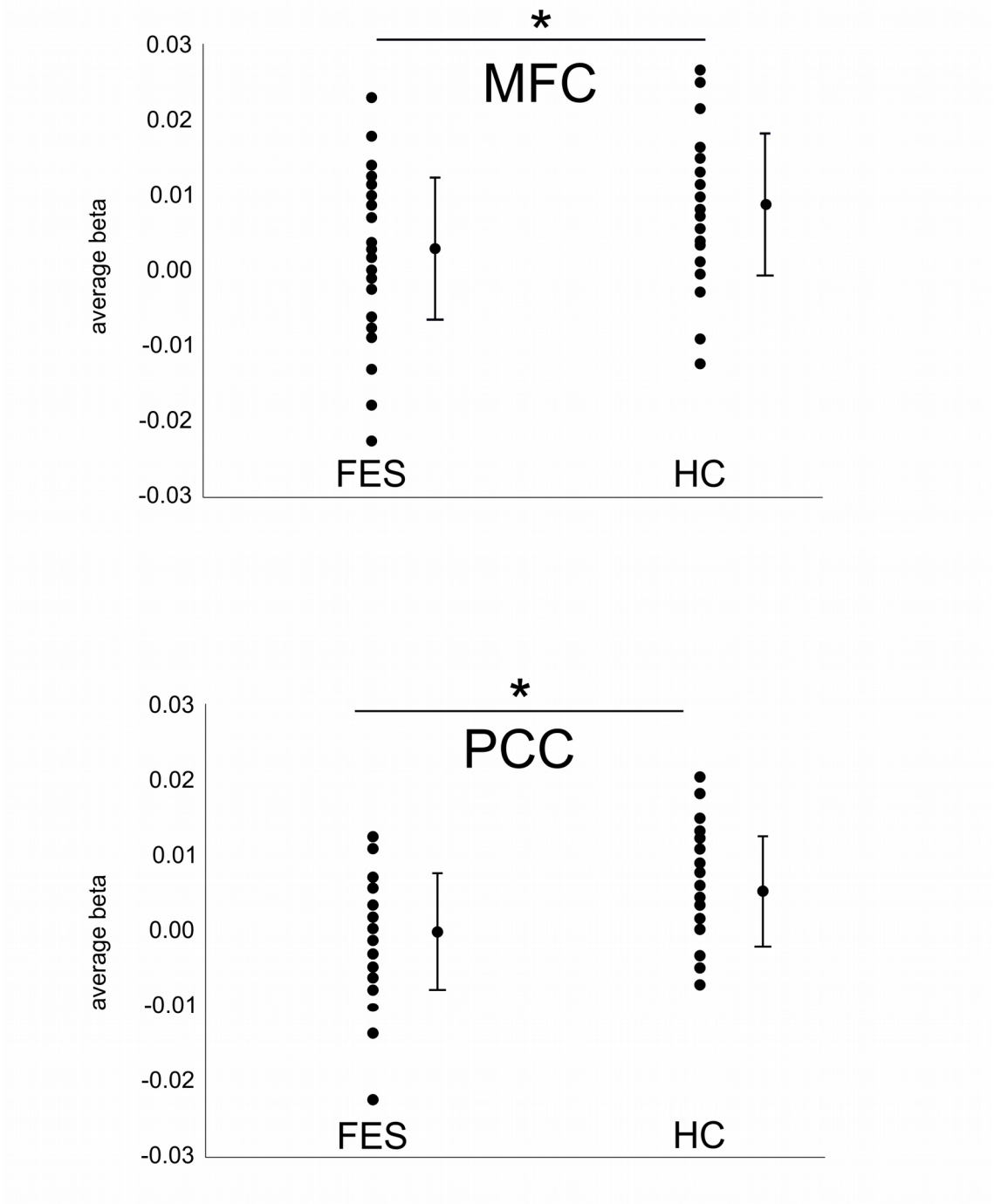

Figure 7. Average beta values (mean, SD) of clusters that are different during self-agency judgment in HC > FES contrast. MFC, mediofrontal cortex. *$P < .01$, *t* test. PCC, posterior cingulate cortex; *$P < .01$, *t* test.

3.2. Resting state functional connectivity

3.2.1. Demographic data

We performed the analysis of the rsFC on the final sample of 63 FES patients and 63 individually age- and sex-matched healthy controls without a personal or a family history of psychiatric disorder. For a detailed description of the samples please see table 3.

3.2.2. Classification of patients and controls

Machine learning applied to rsFC within the SN differentiated FES from the control participants with specificity of 71.4%, sensitivity of 74.6% , and balanced accuracy of 73.0% (p=0.001). In other words, among the 63 FES subjects, 16 individuals were mislabelled as being controls, whereas 18 out of 63 controls were incorrectly classified as FES. The regions which most contributed to the discrimination of the 2 groups contained anterior and posterior cingulate, precuneus, ventro- and dorsolateral prefrontal cortex, angular and supramarginal gyri, temporo-occipital regions, lingular gyrus, and thalamus. The functional connectivity within the other networks, i.e. DMN, CEN, did not yield classifications above chance level, see table 4.

The correctly classified patients did not differ from the misclassified ones in PANSS scores (PANSS Total $t(61)=0.08$, $p=0.9$) or medication dose (CPZ $t(60)=-1.66$, $p=0.1$). There was no association between classification accuracy and CPZ equivalents ($r=-0.21$, $p=0.11$) or symptoms ($r=-0.07$, $p=0.58$). Lastly, ML (GPR) was unable to estimate the chlorpromazine dose ($r=0.22$, $p=0.09$) or the current symptoms as measured by the PANSS total scores or subscales (PANSS Total, $r=-0.03$, $p=0.81$, PANSS Positive, $r=-0.09$, $p=0.472$, PANSS Negative, $r=0.17$, $p=0.184$, PANSS General, $r=-0.03$, $p=0.81$) from the resting state functional connectivity within the SN.

	Controls (n=63)	**Patients (n=63)**	**Note**
Sex – female N (%)	24 (38%)	24 (38%)	
Age, mean (S.D.)	28.1 (6.3)	28.8 (6.2)	t = 0.61; p=0.54
Median duration of illness, months (SD)	n/a	2 (4)*	n/a
Drug dose upon MRI – median chlorpromazine equivalent (SD)	n/a	375 (175)*	n/a
PANSS positive mean (SD)	n/a	16.9 (6.7)	n/a
PANSS negative mean (SD)	n/a	16.9 (6.4)	n/a
PANSS general mean (SD)	n/a	36.3 (9.2)	n/a
PANSS total mean (SD)	n/a	70.1 (17.7)	n/a
* Data from 6 patient missing			

Table 3. Demographic and clinical characteristics of the healthy controls and the patients (rsFC). S.D. – Standard deviation; MRI – Magnetic resonance imaging; PANSS = Positive and negative syndrome scale

ROI	Sensitivity %	*p*	Specificity %	*p*	Balanced accuracy %	*p* (balanced)
posterior cingulate cortex (DMN)	54.0	0.292	57.1	0.155	55.6	p=0.176
dorsolateral prefrontal cortex (CEN)	57.1	0.133	58.7	0.09	57.9	p=0.072
insula anterior (SN)	74.6	0.001	71.4	0.001	73.0	p=0.001

Table 4. The results of the support vector machine classification of patients with a first-episode schizophrenia spectrum disorder and healthy controls from the whole-brain seed-based functional connectivity maps. p values were calculated using permutation testing with 1,000 permutations.

3.2.3. Functional connectivity analysis – between group comparisons

There were no significant differences in whole-brain rsFC between the FES and the control participants on a corrected level for either of the seed regions, i.e. PCC, DLPFC, and SN. We further tested differences in rsFC of the anterior insula on an uncorrected level. The uncorrected comparisons yielded between-group connectivity differences in bilateral angular and supramarginal gyri. These regions closely overlapped with the maximum weight vectors obtained from the ML classification model based on SN connectivity (figure 8).

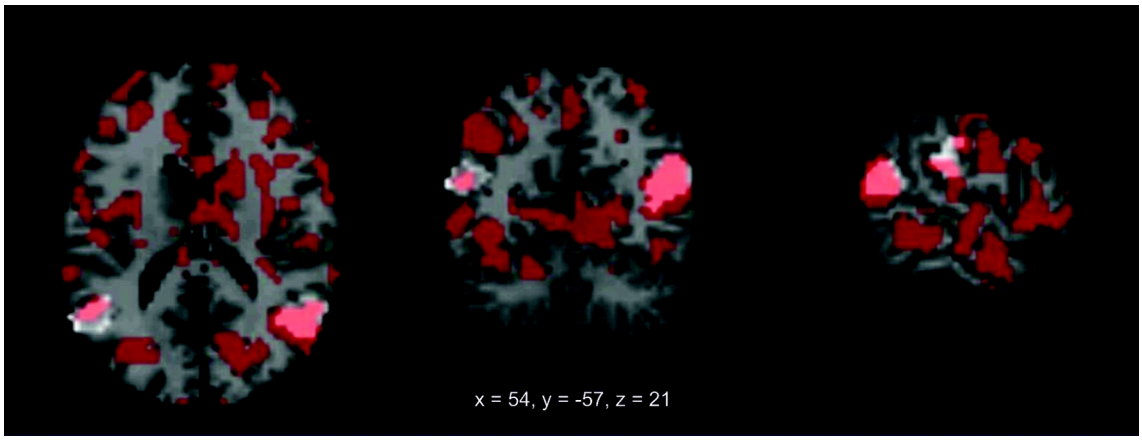

Figure 8. Comparison of the regions contributing to the classification based on salience network connectivity obtained by machine learning (red) with differences between the patients with FES and controls in salience network connectivity (white). Differences in functional connectivity between the patients and the controls were obtained as F-contrast, p=0.001, cluster-level uncorrected.

3.3. DTI

3.3.1. Demographic data

We performed the DTI analysis on the final sample of 77 FES patients and 77 individually age-matched healthy controls without a personal or a family history of psychiatric disorder. For a detailed description of the samples please see table 5.

3.3.2. Classification of patients and controls

The SVM classification yielded statistically significant accuracy of 62.3 % (p=0.005) and specificity of 64.9 % (p=0.005). The sensitivity of 59.7 % did not reach statistical significance (p=0.053). In other words, 46 out of 77 patients were correctly classified as cases, whereas 50 out of 77 healthy controls were correctly classified as controls. The anatomical regions with the highest contribution to the differentiation of FES from controls were diffusely spread along the major white matter tracts, see figure 9A.

The correctly and incorrectly classified patients did not differ in PANSS score, subscale scores or medication dose on the day of scanning (PANSS Total $t(75)=1.39$, $p=0.17$; PANSS Positive, $t(75)=0.96$, $p=0.34$; PANSS Negative, $t(75)=1.52$, $p=0.07$; PANSS General, $t(75)=1.08$, $p=0.14$; CPZ equivalent $t(74)=0.8$, $p=0.43$). There was no association between prediction function value and medication or symptoms (CPZ $r(74)=-0.1$, $p=0.38$; PANSS Total $r(75)=-0.13$, $p=0.26$; PANSS Positive $r(75)=-0.07$, $p=0.56$; PANSS Negative $r(75)=-0.14$, $p=0.24$; PANSS General $r(75)=-0.12$, $p=0.3$). Kernel ridge regression failed to predict either of the clinical variables from the FA (CPZ $r(74)=0.02$, $p=0.29$; PANSS Total $r(75)=-0.15$, $p=0.7$; PANSS Positive $r(75)=-0.34$, $p=0.97$, PANSS Negative $r(75)=0.03$, $p=0.25$; PANSS General $r(75)=-0.15$, $p=0.69$).

	Controls (n=77)	**Patients (n=77)**	**Note**
Sex – female N (%)	34 (44%)	34 (44%)	
Age, mean (S.D.)	28.32 (7.02)	28.51 (7.03)	t = 0.16; p=0.87
Median duration of illness, months (SD)	n/a	3 (7.095)*	n/a
Drug dose upon MRI – median chlorpromazine equivalent (SD)	n/a	337 (234.8)*	n/a
PANSS positive mean (SD)	n/a	13.9 (4.9)	n/a
PANSS negative mean (SD)	n/a	15.7 (6.1)	n/a
PANSS general mean (SD)	n/a	32.8 (8.5)	n/a
PANSS total mean (SD)	n/a	62.4 (16.7)	n/a
* Data from 1 patient missing			

Table 5. Demographic and clinical data of the healthy controls and the patients (DTI). S.D. – Standard Deviation; MRI – Magnetic Resonance Imaging; PANSS = Positive and Negative Syndrome Scale

3.3.3. Statistical analyses of FA differences

Participants with FES showed widespread FA reductions relative to controls (figure 9B). These were contained in a single cluster localized to bilateral tracts of anterior and posterior limbs of the internal capsule, inferior and superior longitudinal fasciculus, inferior fronto-occipital fasciculus, hippocampus, anterior, posterior and superior corona radiata, corpus calossum, cerebral peduncles, inferior, middle cerebellar peduncles and medial lemnisci (size=56647 voxels, maximum differences at x=78, y=84, z=32, corrected p=0.002). We identified no areas where FA was significantly greater in patients than controls. The localization of the between-group differences in FA overlapped with the regions, which contributed to differentiation of FES from control participants on the individual level, see figure 9A, B.

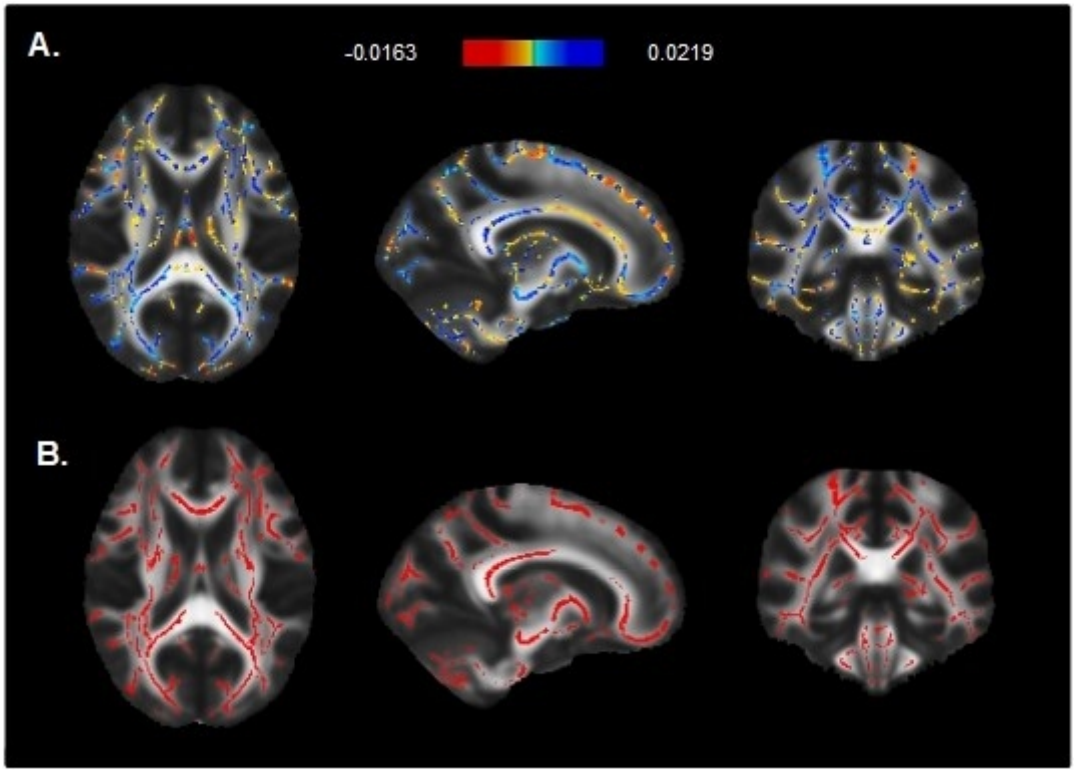

Figure 9. Relative contributions of white-matter regions to the SVM classification and localization of between group differences in FA. A. SVM weight maps for classification of FES and controls. Maximum weights were diffusely distributed across the main white-matter tracts. B. Significant FA differences between FES patients and controls (patients<controls test) ($p<0.05$ FWE corrected, MNI template). The between group differences in FA overlapped with regions which contributed to classification of FES and control participants on individual level.

4. Discussion

In this study, the FES group exhibited a decreased cortical activation during the emergent SA experience within the CMS which is normally involved in SA processing. This yielded significant differences in activation during SA recognition using a classical between-group comparison, reflecting a biological correlate of FES. However, this finding lacks a potential clinical utility, which is illustrated by the large overlap of the magnitudes of differences between the FES group and the control group. On the other hand, ML applied to the whole-brain rsFC maps of the anterior insula/SN differentiated FES participants from controls on the indifidual level with an above chance accuracy of 73% (p=0.001). Similarly, whole brain FA maps differentiated patients with FES and healthy controls with above chance accuracy of 62.3 % (p=0.005). In both analyses, the classification was mostly based on voxels that overlapped with the between-group differences obtained by conventional statistics (see figures 7, 8A,B). The classification was not significantly affected by the medication dose, or by the presence of psychotic symptoms, and thus was likely based on trait rather than state markers.

4.1. fMRI analysis using classical between group comparisons

To illustrate the differences in methodological and interpretational aspects between classical statistical analysis and machine learning, we used a block design paradigm and analyzed it using classical between group comparisons (two-sample T-test). In the SA/OA task we identified significant differences in activations between patients and controls in the medial frontal gyrus and the posterior cingulate gyrus (table 2, figure 6). These results were in accordance with previous literature that attributed the self-agency processing to the CMS structures. The clusters were highly significant on the family-wise error corrected level (P value $\leq .05$). However, on the individual level there was a high overlap of the individual beta estimates within the clusters (figure 7). This illustrates the common limitation of the neuroimaging studies. The statistical inference allowed us to identify the biological marker of FES on a group level, however, due to the low effect size of the observed differences this study cannot assist in clinical decisions which have to be personalized on the level of single subjects.

4.2. Classification accuracy using rsFC and FA

Our further analyses usind ML provide a proof of concept that resting state fMRI and FA can be successfully used to differentiate participants with FES from healthy controls. rsfMRI is particularly suitable for diagnostic classification (Craddock et al., 2009; Haller et al., 2014). Compared to task based fMRI paradigms, the resting state approach reduces the amount of bias introduced by task non-adherence. This is an important advantage in participants with FES, who tend to have distorted perception and impaired cognitive functioning. Also the rsFC seed regions can be selected *á priori* from pre-defined atlases, which makes this approach transferable among independent groups of subjects.

Although it is difficult to directly compare the results of our analyses to the previously published work due to the methodological differences, the classification performance obtained using rsFC in this study was comparable to the sensitivity and specificity obtained from structural MRI and rsfMRI in established schizophrenia and FES on a meta-analytical level Kambeitz et al. (2015) (sensitivity 76% and specificity 79% for structural MRI, sensitivity 84% and specificity 77% for rsfMRI). Individual studies that focused on FES exclusively have reported accuracies ranging from 54% to 90 % for structural MRI (Kasparek et al., 2011; Pettersson-Yeo et al., 2013; Zanetti et al., 2013).

In the case of FA, although our results support the potential diagnostic utility in FES as well, the overall accuracy of classification was relatively low. This could be related to the type of MRI modality, i.e. the use of DTI, or the clinical population, i.e. FES, who may show a lower extent of abnormalities than participants with chronic, long standing illness. Although direct comparison is not possible due to methodological heterogeneity, previous studies using ML and DTI suggest, that DTI gives generally lower prediction accuracies in FES (Pettersson-Yeo et al., 2013; Zanetti et al., 2013).

Overall, there seems to be a general trend towards higher prediction accuracies in chronic stages of disease, as the meta-analysis by Kambeitz et al. (2015) shows, which might reflect the higher prevalence of structural/functional changes due to the disease progression.

4.3. ML versus between-group statistics

While the SVM was able to extract enough information from the rsFC to classify patients and controls on the individual level, the between-group differences in the aINS connectivity did not reach statistical significance. However, on an uncorrected level, the localisation of between-group differences overlapped with the regions with a maximum contribution to the classification using ML. Due to the multivariate nature, which obviates the need to control for multiple comparisons, ML appears to be more sensitive than conventional mass univariate approaches and thus being able to make significant predictions on the individual level.

Whereas in the classification based on rsFC, SVM classification was more sensitive than between group analysis, in the analysis of DTI data, there was a discrepancy between the high significance of between-group differences and a relatively low prediction accuracy obtained by machine learning. Surprisingly, we found marked and diffuse differences in FA between FES and controls when using standard methods of between group comparisons. This may be related to the type of ML analyses, feature selection, SVM settings, which may alter the sensitivity of the analyses. As our intentions were clinical, we used a simple, standardized approach potentially suitable for clinical application. Having to fine tune the analyses to specific sample would complicate clinical utility. The “out of the box” approach appears to work well for structural MRI (Mourao-Miranda et al., 2012). Perhaps DTI analyses require different default settings or different machine learning algorithms, such as random forest or discriminant analyses. Fine-tuning the SVM models to DTI or finding a ML algorithm better suited for DTI analyses, is beyond the scope of this article, but would be a rich topic for future methodological research.

4.4. Implications for the neurobiology of FES

4.4.1. Anterior insula and salience network

The classification of FES and HC using rsFC was significant when the connectivity of anterior insula was used. The anterior insula is a crucial component of the SN. The

disruption of aINS and SN connectivity has been well documented in schizophrenia (Iwabuchi et al., 2015; Manoliu et al., 2014; Palaniyappan et al., 2013b; White et al., 2010). Additionally, a grey matter reduction within the insula has been consistently and robustly reported in the meta-analyses of morphometric MRI studies of schizophrenia (Bora et al., 2011; Ellison-Wright and Bullmore, 2010; Glahn et al., 2008; Palaniyappan et al., 2013). However, the specificity of these changes to schizophrenia is unclear. Recent findings suggest that a general mapping exists between a broad range of psychiatric symptoms and the integrity of an anterior insula-based network across a wide variety of neuropsychiatric illnesses (Goodkind et al., 2015).

Although DMN and CEN exhibit functional abnormalities in schizophrenia (Ren et al., 2013; Spaniel et al., 2016) we did not achieve above chance classifications when we focused on connectivity within these networks. We also did not identify any significant between-group functional connectivity differences in these networks. One explanation may lie in the dynamics of structural brain changes during the course of an illness. Some studies suggest that insular cortex grey matter abnormalities in psychotic disorders may reflect pre-existing vulnerability. Later in the course of an illness, the changes secondary to the illness burden, may lead to the extension of these alterations to other neighbouring structures (Chan et al., 2011; Takahashi et al., 2009). However, other studies do not support this view of dynamic pattern changes in brain morphology (Vita et al., 2012).

Another explanation is that previous findings reflect clinical heterogeneity vis-a-vis the clinical course. Recent studies have demonstrated that classification accuracies are higher in participants with chronic course of illness, and lower in those with an episodic illness. Perhaps the presence of patients who will go on to develop an episodic illness could have decreased the prediction accuracies for some of the networks (Gould et al., 2014; Mourao-Miranda et al., 2012).

4.4.2. Between-group FA differences in FES

We replicated previous findings showing that white matter alterations in FES are diffuse and not localized (Alvarado-Alanis et al., 2015; Bora et al., 2011; Kelly et al., 2017). In

keeping with this, the machine learning algorithm used diffuse patterns of white matter changes to identify FES participants (figure 9). In all instances lower FA values were associated with the diagnosis of FES. Lower FA may indicate that white matter tracts are less organized, have lower density, lower degree of myelination, more crossing fibers or that the membranes are more permeable (Jones et al., 2013). Overall, these findings support the growing evidence suggesting disruption of white matter microstructure in FES, which could possibly be used diagnostically.

5. Limitations

A common problem in machine learning is overfitting (Whelan and Garavan, 2014). In general, when the number of features exceeds the number of subjects, classifiers can underperform due low ability to generalize because of overfitting of the model to the training dataset (Pereira et al., 2009). We used a linear-kernel SVM classifier, which was shown to have a low likelihood of overfitting in fMRI paradigms (LaConte et al., 2005; Mourao-Miranda et al., 2012). In addition, in the analysis of the rsFC two out of three of our models failed to produce significant results, which makes overfitting in this analysis unlikely.

One potential explanation for the observed low accuracy in the case of our analysis of the FA may be the relatively high complexity of the fitted model, related to the very high dimension of the data, with number of features three orders of magnitude higher than the number of subjects. This was reflected in the high number of support vectors in the model (in most folds of the cross-validation scheme, 152 support vectors (SV) were used by the SVM, i.e. all data points had the role of SV). On the other hand, SVM algorithm is generally suitable for working with high-dimensional data and is robust against irrelevant features (Nilsson et al., 2006). The high number of SV does not necessarily imply overfitting, but can be rather a natural consequence of high data dimensionality.

Unlike the healthy controls, all of the patients were on antipsychotic medication and experienced mild psychotic symptoms at the time of scanning. There are a limited number of studies focusing on correlations of clinical symptom severity and/or medication dose with resting FC in FES. The results differ depending on the regions of interest. Some studies have found positive as well as negative correlations of striatal connectivity with symptom severity that was resolved with treatment (Sarpal et al., 2015). However, another study reported no correlations between symptom severity and a resting FC of DMN (Alonso-Solís et al., 2012). So both symptoms and medications might potentially confound the results (Kambeitz et al., 2015). However, there was no significant association between symptoms or medication dose and classification accuracy. Likewise, ML was unable to estimate symptom levels or medication dose

from the rsFC and DTI data. Last but not least, there were no significant differences between the correctly and incorrectly classified subjects in symptom levels or medication dose. Thus, it is unlikely that medication or psychotic symptoms markedly contributed to the classification.

As this is an emerging field, there is no standardization of the methods of data preprocessing and analyses for the machine learning studies. Of course, a range of alternative classification procedures could be applied, including various dimensionality reduction methods combined with more complex models, starting from kernel SVM variants. However, methodological advances of SVM were not our objective. We do not know exactly the influence of individual processing steps or selection of ROI on the outcomes. At the same time, the SVMs are among the longest and most used ML classifiers in psychiatric neuroimaging (Arbabshirani et al., 2014; Sundermann et al., 2014). Consequently, we used SVM with the default parameters in order to decrease the methodological heterogeneity and to ensure comparability with other studies. This way, we showed that even a simple, easily applicable classifier with linear (hyperplane) decision boundary could correctly distinguish between patients and controls. For the same reason, we used standard atlases to select the ROIs, which are representative of the individual RSNs. In the case of DTI, we used a standardized whole-brain pre-processing of the FA (TBSS, see Methods section).

6. Future perspectives

Future studies should attempt to use this approach in unaffected individuals at a genetic risk of schizophrenia, should aim to test the specificity of the results to schizophrenia and might benefit from novel classification algorithms. Further methodological attempts should be taken to perform individualized predictions regarding the prognosis or choice of therapeutic interventions, or to identify unknown subpopulations of patients using machine learning.

6.1. Multimodal classification

Currently it is not known which modality is the most suitable for classification studies. Our studies show that some modalities might provide superior information to others. For example, FA was not as effective as the rsFC. One approach to extract the highest amount of information from brain scans is to use multiple modalities. Some authors propose this approach might improve the classification performance (Cabral et al., 2016; Peruzzo et al., 2014).

6.2. Personalised medicine

The majority of classification studies have focused on differentiating between two groups - patients and controls. This might be relevant in a preselected group of patients, such as clients of high risk outpatient clinics already exhibiting some psychotic symptoms. However, real clinical questions can be more complicated. A clinician may find himself in a situation when he should make a differential diagnosis between more disorders such as between schizophrenia, bipolar or personality disorder. For such decision making the classifier should be able to differentiate between many groups of psychiatric disorders. One such example migt be a classification between schizophrenia and mood disorders (Koutsouleris et al., 2015). Although the approach of these authors does not directly imply a between diagnostic classification, it suggests that differences of structural patterns can provide information about the differences between the disorders on the individual level.

Another important decision that a clinical psychiatrist has to make is treatment choice. In the absence of clinically relevant biomarkers this is usually done in a trial and error manner. It takes several weeks to be able to assess the therapeutic response. If the first medication fails, medications are typically changes, which required another several weeks to assess response. This results in extremely long time spent in the episode of mental illness which may be accompanied with potential harms such as chronification or increased risk of suicide. Several authors have tried to predict the therapeutic outcome with machine learning from neuroimaging data. Such a tool might have a tremendous effect on the clinical psychiatric practice reducing the time spent in wards, number of visits in outpatient clinics or in general time spent in disability, as well as improve the therapeutic outcomes and the quality of life of psychiatric patients (Koutsouleris et al., 2017).

Personalized decision making in medicine is definitely extremely difficult to achieve. On the other hand, the research towards the so-called precision medicine seems to be based on actual and realistic findings. Unlike personalized medicine, precision medicine aims at selecting the treatment that is most likely to work according to specific biomarkers. In line with this, with this several studies have found distinct subtypes of disorders within the existing diagnoses such as 2 subtypes of depression or deficit/non deficit schizophrenia (Lamers et al., 2017; Voineskos et al., 2013). The NIMH Research Domain Criteria (RDoC) initiative (Cuthbert and Insel, 2013) provided an interesting framework for re-thinking the existing diagnostic categories in terms of neuroscience informed and biologically relevant terms (Casey et al., 2013). The given biological constructs (e.g. auditory perception) could be specifically targeted (auditory oddball paradigm) and used as biomarkers for prediction of symptom severity in schizophrenia (Gheiratmand et al., 2017).

6.3. Big data model

Acquiring large amounts of data within multicenter studies will not only increase the statistical power but more importantly, allow us to look for multivariate relationships in order to identify previously unknown subgroups within existing diagnostic entities by unsupervised machine learning methods or develop predictive models for precision

medicine using supervised learning (Milham et al., 2017; Varoquaux and Craddock, 2013).

Prediction models based on the data sets from one site tend to suffer from low generalizability on datasets from different sites. One approach to address this issue is to use a subsample of recruited population to validate the trained ML models on "unseen" data. The problem with this approach is, that both train and validation samples come from the same populations such as clinical or research trials and the data acquisition is performed in the same conditions being specific for the given study or clinic. Therefore, such classifiers might poorly generalize to other populations examined in different clinics, using different scanners etc. Larger datasets need to be acquired not only to increase the size of training sets, but also allow for the external validation of trained models (Iniesta et al., 2016; Schnack et al., 2010).

A current common solution seems to be repurposing previously collected data within multicenter consortia, such as as ENIGMA, (the Alzheimer's Disease Neuroimaging Initiative, EPIGEN Consortium, IMAGEN Consortium, Saguenay Youth Study (SYS) Group et al., 2014). Unfortunately, analyses of such pooled datasets are complicated not only due to technical issues (e.g. different scanner types, high computation power), but also legal and ethical issues (sharing of sensitive information about patients and controls). To overcome these, (Dluhoš et al., 2017) developed a solution, which allows sharing and combining SVM models trained on individual data sets from different sites. The combined meta-model was comparably accurate as the model trained on a pooled sample. An important advantage of this approach is, that it requires only sharing of the computed meta-models rather than sensitive patients' information.

In contrast to large, shallowly phenotyped studies with broad definitions of illness, there has also been an increasing need to focus on well characterized, more homogeneous samples of patients. Focusing on more homogeneous categories defined by symptoms, clinical course or response to treatment and controlling for relevant confounders already in the design of the study still provides the best tool to search for the effective interventions or to characterize specific clinical subgroups within the broadly defined diagnostic categories (Hajek et al., 2015; Propper et al., 2015; Rao et al., 2017).

6.4. Early diagnosis of schizophrenia – first episode or psychosis risk syndrome?

Since late 1980 there has been an increasing initiative to capture the developing schizophrenia already in its prodromal phase (Huber and Gross, 1989). It was shown, that the majority of patients exhibit prodromal symptoms already up to 5 years before the disease onset (Häfner et al., 1998). This so called "at-risk mental state" or "ultra-high-risk" syndrome (UHR) has been defined according to several complementary sets of criteria with slightly different ability to capture the phase of the of the UHR (Fusar-Poli et al., 2013). The transition to psychosis occurs in 18% at 1 year follow-up to 39% at 3 years follow-up (Fusar-Poli et al., 2012). Specialized treatment services were created predominantly in Australia, Great Britain and Germany, where the focused treatment, which includes the CBT and fish oil supplements decreased the transition risk (Preti and Cella, 2010).

From the prevention point of view, detecting the psychosis onset at the UHR level seems to be even better than at the onset of the FES. On the other hand, in a recent study only a minority of patients presenting with FES (4.1%) came from the prodromal services (Ajnakina et al., 2017). The majority of patients still enter the health care services at the point of the first episode. Therefore, in spite of the fascinating possibilities the UHR concept introduced, the FES is the point where the most of the clinical decision-making takes part.

7. Conclusions

To conclude, this study provides a proof of concept that ML applied both to the seed-based rsFC maps and whole brain FA values may help differentiate patients early in the course of schizophrenia from healthy controls on an individual level, even when using a relatively simple, "out of the box" machine learning classifier. We were able to discriminate patients with FES from healthy controls with an accuracy of 73% (rsFC) and 62.3% (DTI). The classification was probably based on trait rather than state markers, as symptoms or medications were not significantly associated with classification accuracy. Furthermore, our results emphasise the role of resting-state connectivity within the SN in the pathophysiology of FES. Although the classification based on the FA performed above the chance level, the accuracy was relatively low. Yet, the TBSS analyses showed marked differences in FA between FES and controls. Due to this discrepancy, it is possible that a different ML algorithm might improve the classification accuracy.

8. Shrnutí

V této práci jsme ukázali, že s využitím relativně jednoduchého ML klasifikátoru je možné odlišit na individuální úrovni pacienty s FES od zdravých dobrovolníků z dat seed-based klidové funkční konektivity i frakční anizotropie. Pacienty s FES jsme klasifikovali s přesností klasifikace 73% (rsFC) a 62.3% (DTI). Klasifikace reflektuje spíše ‘’trait’’ nežli ‘’state’’ markry onemocnění, protože nebyla statisticky asociována s mírou symptomy ani dávkou medikace. Výsledky analýzy rsFC a fMRI během prožitku‘‘self-agency‘‘ na meziskupinové úrovni poukazují na význam přední inzuly/salience network a CMS v patofyziologii FES. Přestože klasifikace založená na FA dosáhla statistické významnosti, přesnost klasifikace byla relativně nízká. Analýza TBSS však ukázala výrazné rozdíly v FA mezi FES a kontrolami. Je možné, že jiný ML algoritmus může zlepšit přesnost klasifikace, optimalizace algorytmu ale nebyla cílem naší ‘‘proof of concept‘‘ analýzy.

9. List of abbreviations

aINS - anterior insula

BA - Brodmann area

BOLD - blood oxygen-level dependent signal

CEN - central executive network

CPZ - chlorpromazine equivalent

CMS - central midline structures

DMN - default mode network

DLPFC - dorsolateral prefrontal cortex

DTI - diffusion tensor imaging

FA - fractional anisotropy

FES - first episode of schizophrenia-spectrum disorder

fMRI - functional magnetic resonance imaging

GPR - Gaussian process regression

HC - healthy control subjects

KR - kernel ridge regression

ML - machine learning

MRI – Magnetic Resonance Imaging

OA - "other" agency

PANSS - positive and negative syndrome scale

RDoC - research domain criteria

rsFC - resting state functional connectivity

rsfMRI - resting-state functional MRI

RSNs - resting state networks

SA - "self" agency

SN - salience network

SVM - support-vector machine

TBSS - tract based spatial statistics

TEVS - target events

TFCE - threshold free cluster enhancement

UHR - ultra high risk state

11. References

Ajnakina, O., Morgan, C., Gayer-Anderson, C., Oduola, S., Bourque, F., Bramley, S., Williamson, J., MacCabe, J.H., Dazzan, P., Murray, R.M., David, A.S., 2017. Only a small proportion of patients with first episode psychosis come via prodromal services: a retrospective survey of a large UK mental health programme. BMC Psychiatry 17. https://doi.org/10.1186/s12888-017-1468-y

Allen, L.M., Hasso, A.N., Handwerker, J., Farid, H., 2012. Sequence-specific MR Imaging Findings That Are Useful in Dating Ischemic Stroke. RadioGraphics 32, 1285–1297. https://doi.org/10.1148/rg.325115760

Alonso-Solís, A., Corripio, I., de Castro-Manglano, P., Duran-Sindreu, S., Garcia-Garcia, M., Proal, E., Nuñez-Marín, F., Soutullo, C., Alvarez, E., Gómez-Ansón, B., al, et, 2012a. Altered default network resting state functional connectivity in patients with a first episode of psychosis. Schizophr. Res. 139, 13–18. https://doi.org/10.1016/j.schres.2012.05.005

Alonso-Solís, A., Corripio, I., de Castro-Manglano, P., Duran-Sindreu, S., Garcia-Garcia, M., Proal, E., Nuñez-Marín, F., Soutullo, C., Alvarez, E., Gómez-Ansón, B., Kelly, C., Castellanos, F.X., 2012b. Altered default network resting state functional connectivity in patients with a first episode of psychosis. Schizophr. Res. 139, 13–18. https://doi.org/10.1016/j.schres.2012.05.005

Alvarado-Alanis, P., León-Ortiz, P., Reyes-Madrigal, F., Favila, R., Rodríguez-Mayoral, O., Nicolini, H., Azcárraga, M., Graff-Guerrero, A., Rowland, L.M., de la Fuente-Sandoval, C., 2015. Abnormal white matter integrity in antipsychotic-naïve first-episode psychosis patients assessed by a DTI principal component analysis. Schizophr. Res. 162, 14–21. https://doi.org/10.1016/j.schres.2015.01.019

Amarreh, I., Meyerand, M.E., Stafstrom, C., Hermann, B.P., Birn, R.M., 2014. Individual classification of children with epilepsy using support vector machine with multiple indices of diffusion tensor imaging. NeuroImage Clin. 4, 757–764. https://doi.org/10.1016/j.nicl.2014.02.006

Andreasen, N.C., Nopoulos, P., Magnotta, V., Pierson, R., Ziebell, S., Ho, B.-C., 2011. Progressive brain change in schizophrenia: a prospective longitudinal study of first-episode schizophrenia. Biol. Psychiatry 70, 672–679. https://doi.org/10.1016/j.biopsych.2011.05.017

Arbabshirani, M.R., Castro, E., Calhoun, V.D., 2014. Accurate classification of schizophrenia patients based on novel resting-state fMRI features. IEEE, pp. 6691–6694. https://doi.org/10.1109/EMBC.2014.6945163

Biswal, B., Yetkin, F.Z., Haughton, V.M., Hyde, J.S., 1995. Functional connectivity in the motor cortex of resting human brain using echo-planar MRI. Magn. Reson. Med. 34, 537–541.

Biswal, B.B., 2012. Resting state fMRI: A personal history. NeuroImage, 20 YEARS OF fMRI 62, 938–944. https://doi.org/10.1016/j.neuroimage.2012.01.090

Bora, E., Fornito, A., Radua, J., Walterfang, M., Seal, M., Wood, S.J., Yücel, M., Velakoulis, D., Pantelis, C., 2011. Neuroanatomical abnormalities in schizophrenia: A multimodal voxelwise meta-analysis and meta-regression analysis. Schizophr. Res. 127, 46–57. https://doi.org/10.1016/j.schres.2010.12.020

Bressler, S.L., Menon, V., 2010. Large-scale brain networks in cognition: emerging methods and principles. Trends Cogn. Sci. 14, 277–290. https://doi.org/10.1016/j.tics.2010.04.004

Brodersen, K.H., Deserno, L., Schlagenhauf, F., Lin, Z., Penny, W.D., Buhmann, J.M., Stephan, K.E., 2014. Dissecting psychiatric spectrum disorders by generative embedding. NeuroImage Clin. 4, 98–111. https://doi.org/10.1016/j.nicl.2013.11.002

Cabral, C., Kambeitz-Ilankovic, L., Kambeitz, J., Calhoun, V.D., Dwyer, D.B., von Saldern, S., Urquijo, M.F., Falkai, P., Koutsouleris, N., 2016. Classifying Schizophrenia Using Multimodal Multivariate Pattern Recognition Analysis: Evaluating the Impact of Individual Clinical Profiles on the Neurodiagnostic Performance. Schizophr. Bull. 42, S110–S117. https://doi.org/10.1093/schbul/sbw053

Cabral, J., Kringelbach, M.L., Deco, G., 2014. Exploring the network dynamics underlying brain activity during rest. Prog. Neurobiol. 114, 102–131. https://doi.org/10.1016/j.pneurobio.2013.12.005

Canu, E., Agosta, F., Filippi, M., 2015. A selective review of structural connectivity abnormalities of schizophrenic patients at different stages of the disease. Schizophr. Res., White Matter Pathology 161, 19–28. https://doi.org/10.1016/j.schres.2014.05.020

Casey, B.J., Craddock, N., Cuthbert, B.N., Hyman, S.E., Lee, F.S., Ressler, K.J., 2013. DSM-5 and RDoC: progress in psychiatry research? Nat. Rev. Neurosci. 14, 810–814. https://doi.org/10.1038/nrn3621

Castellanos, F.X., Di Martino, A., Craddock, R.C., Mehta, A.D., Milham, M.P., 2013. Clinical applications of the functional connectome. NeuroImage 80, 527–540. https://doi.org/10.1016/j.neuroimage.2013.04.083

Chaiyakunapruk, N., Chong, H.Y., Teoh, S.L., Wu, D.B.-C., Kotirum, S., Chiou, C.-F., 2016. Global economic burden of schizophrenia: a systematic review. Neuropsychiatr. Dis. Treat. 357. https://doi.org/10.2147/NDT.S96649

Chan, R.C.K., Di, X., McAlonan, G.M., Gong, Q., 2011. Brain anatomical abnormalities in high-risk individuals, first-episode, and chronic schizophrenia: an activation likelihood estimation meta-analysis of illness progression. Schizophr. Bull. 37, 177–188. https://doi.org/10.1093/schbul/sbp073

Chao-Gan, Y., Yu-Feng, Z., 2010. DPARSF: A MATLAB Toolbox for "Pipeline" Data Analysis of Resting-State fMRI. Front. Syst. Neurosci. 4, 13. https://doi.org/10.3389/fnsys.2010.00013

Craddock, R.C., Holtzheimer, P.E., Hu, X.P., Mayberg, H.S., 2009. Disease state prediction from resting state functional connectivity. Magn. Reson. Med. Off. J. Soc. Magn. Reson. Med. Soc. Magn. Reson. Med. 62, 1619–1628. https://doi.org/10.1002/mrm.22159

Cuthbert, B.N., Insel, T.R., 2013. Toward the future of psychiatric diagnosis: the seven pillars of RDoC. BMC Med. 11, 126. https://doi.org/10.1186/1741-7015-11-126

Damoiseaux, J.S., Rombouts, S. a. R.B., Barkhof, F., Scheltens, P., Stam, C.J., Smith, S.M., Beckmann, C.F., 2006. Consistent resting-state networks across healthy subjects. Proc. Natl. Acad. Sci. 103, 13848–13853. https://doi.org/10.1073/pnas.0601417103

Destrieux, C., Fischl, B., Dale, A., Halgren, E., 2010. Automatic parcellation of human cortical gyri and sulci using standard anatomical nomenclature. NeuroImage 53, 1–15. https://doi.org/10.1016/j.neuroimage.2010.06.010

Dluhoš, P., Schwarz, D., Cahn, W., van Haren, N., Kahn, R., Španiel, F., Horáček, J., Kašpárek, T., Schnack, H., 2017. Multi-center machine learning in imaging psychiatry: A meta-model approach. NeuroImage 155, 10–24. https://doi.org/10.1016/j.neuroimage.2017.03.027

Dong, Q., Welsh, R.C., Chenevert, T.L., Carlos, R.C., Maly-Sundgren, P., Gomez-Hassan, D.M., Mukherji, S.K., 2004. Clinical applications of diffusion tensor imaging. J. Magn. Reson. Imaging 19, 6–18. https://doi.org/10.1002/jmri.10424

Doughty, C., Wang, J., Feng, W., Hackney, D., Pani, E., Schlaug, G., 2016. Detection and Predictive Value of Fractional Anisotropy Changes of the Corticospinal Tract in the Acute Phase of a Stroke. Stroke 47, 1520–1526. https://doi.org/10.1161/STROKEAHA.115.012088

Dwyer, D.B., Falkai, P., Koutsouleris, N., 2018. Machine Learning Approaches for Clinical Psychology and Psychiatry. Annu. Rev. Clin. Psychol. 14, 91–118. https://doi.org/10.1146/annurev-clinpsy-032816-045037

Ellison-Wright, I., Bullmore, E., 2010. Anatomy of bipolar disorder and schizophrenia: A meta-analysis. Schizophr. Res. 117, 1–12. https://doi.org/10.1016/j.schres.2009.12.022

Farrer, C., Franck, N., Frith, C.D., Decety, J., Georgieff, N., d'Amato, T., Jeannerod, M., 2004. Neural correlates of action attribution in schizophrenia. Psychiatry Res. 131, 31–44. https://doi.org/10.1016/j.pscychresns.2004.02.004

Fischl, B., Salat, D.H., van der Kouwe, A.J.W., Makris, N., Ségonne, F., Quinn, B.T., Dale, A.M., 2004. Sequence-independent segmentation of magnetic resonance images. NeuroImage 23 Suppl 1, S69-84. https://doi.org/10.1016/j.neuroimage.2004.07.016

Fletcher, P.C., Frith, C.D., 2009. Perceiving is believing: a Bayesian approach to explaining the positive symptoms of schizophrenia. Nat. Rev. Neurosci. 10, 48–58. https://doi.org/10.1038/nrn2536

Franke, K., Ziegler, G., Klöppel, S., Gaser, C., 2010. Estimating the age of healthy subjects from T1-weighted MRI scans using kernel methods: Exploring the influence of various parameters. NeuroImage 50, 883–892. https://doi.org/10.1016/j.neuroimage.2010.01.005

Fusar-Poli, P., Bonoldi, I., Yung, A.R., Borgwardt, S., Kempton, M.J., Valmaggia, L., Barale, F., Caverzasi, E., McGuire, P., 2012. Predicting psychosis: meta-analysis of transition outcomes in individuals at high clinical risk. Arch. Gen. Psychiatry 69, 220–229. https://doi.org/10.1001/archgenpsychiatry.2011.1472

Fusar-Poli, P., Borgwardt, S., Bechdolf, A., Addington, J., Riecher-Rössler, A., Schultze-Lutter, F., Keshavan, M., Wood, S., Ruhrmann, S., Seidman, L.J., Valmaggia, L., Cannon, T., Velthorst, E., De Haan, L., Cornblatt, B., Bonoldi, I., Birchwood, M., McGlashan, T., Carpenter, W., McGorry, P., Klosterkötter, J., McGuire, P., Yung, A., 2013. The Psychosis High-Risk State. JAMA Psychiatry 70, 107–120. https://doi.org/10.1001/jamapsychiatry.2013.269

Fusar-Poli, P., Politi, P., 2008. Paul Eugen Bleuler and the Birth of Schizophrenia (1908). Am. J. Psychiatry 165, 1407–1407. https://doi.org/10.1176/appi.ajp.2008.08050714

Gheiratmand, M., Rish, I., Cecchi, G.A., Brown, M.R.G., Greiner, R., Polosecki, P.I., Bashivan, P., Greenshaw, A.J., Ramasubbu, R., Dursun, S.M., 2017. Learning stable and predictive network-based patterns of schizophrenia and its clinical symptoms. Npj Schizophr. 3, 22. https://doi.org/10.1038/s41537-017-0022-8

Glahn, D.C., Laird, A.R., Ellison-Wright, I., Thelen, S.M., Robinson, J.L., Lancaster, J.L., Bullmore, E., Fox, P.T., 2008. Meta-Analysis of Gray Matter Anomalies in Schizophrenia: Application of Anatomic Likelihood Estimation and Network Analysis. Biol. Psychiatry 64, 774–781. https://doi.org/10.1016/j.biopsych.2008.03.031

Goodkind, M., Eickhoff, S.B., Oathes, D.J., Jiang, Y., Chang, A., Jones-Hagata, L.B., Ortega, B.N., Zaiko, Y.V., Roach, E.L., Korgaonkar, M.S., Grieve, S.M., Galatzer-Levy, I., Fox, P.T., Etkin, A., 2015. Identification of a Common Neurobiological Substrate for Mental Illness. JAMA Psychiatry 72, 305. https://doi.org/10.1001/jamapsychiatry.2014.2206

Gould, I.C., Shepherd, A.M., Laurens, K.R., Cairns, M.J., Carr, V.J., Green, M.J., 2014. Multivariate neuroanatomical classification of cognitive subtypes in schizophrenia: a support vector machine learning approach. NeuroImage Clin. 6, 229–236. https://doi.org/10.1016/j.nicl.2014.09.009

Greicius, M.D., Krasnow, B., Reiss, A.L., Menon, V., 2003. Functional connectivity in the resting brain: a network analysis of the default mode hypothesis. Proc. Natl. Acad. Sci. U. S. A. 100, 253–258. https://doi.org/10.1073/pnas.0135058100

Guo, W., Xiao, C., Liu, G., Wooderson, S.C., Zhang, Z., Zhang, J., Yu, L., Liu, J., 2014. Decreased resting-state interhemispheric coordination in first-episode, drug-naive paranoid schizophrenia. Prog. Neuropsychopharmacol. Biol. Psychiatry 48, 14–19. https://doi.org/10.1016/j.pnpbp.2013.09.012

Guo, X., Li, J., Wei, Q., Fan, X., Kennedy, D.N., Shen, Y., Chen, H., Zhao, J., 2013. Duration of Untreated Psychosis Is Associated with Temporal and Occipitotemporal Gray Matter Volume Decrease in Treatment Naïve Schizophrenia. PLoS ONE 8, e83679. https://doi.org/10.1371/journal.pone.0083679

Häfner, H., Maurer, K., Löffler, W., an der Heiden, W., Munk-Jørgensen, P., Hambrecht, M., Riecher-Rössler, A., 1998. The ABC Schizophrenia Study: a preliminary overview of the results. Soc. Psychiatry Psychiatr. Epidemiol. 33, 380–386.

Hajek, T., Bauer, M., Pfennig, A., Cullis, J., Ploch, J., O'Donovan, C., Bohner, G., Klingebiel, R., Young, L., MacQueen, G., Alda, M., 2012. Large positive effect of lithium on prefrontal cortex N-acetylaspartate in patients with bipolar disorder: 2-centre study. J. Psychiatry Neurosci. 37, 185–192. https://doi.org/10.1503/jpn.110097

Hajek, T., Cooke, C., Kopecek, M., Novak, T., Hoschl, C., Alda, M., 2015. Using structural MRI to identify individuals at genetic risk for bipolar disorders: a 2-cohort, machine learning study. J. Psychiatry Neurosci. JPN 40, 316–324.

Hajek, T., Franke, K., Kolenic, M., Capkova, J., Matejka, M., Propper, L., Uher, R., Stopkova, P., Novak, T., Paus, T., Kopecek, M., Spaniel, F., Alda, M., 2017. Brain Age in Early Stages of Bipolar Disorders or Schizophrenia. Schizophr. Bull. https://doi.org/10.1093/schbul/sbx172

Haller, S., Badoud, S., Nguyen, D., Garibotto, V., Lovblad, K.O., Burkhard, P.R., 2012. Individual detection of patients with Parkinson disease using support vector machine analysis of diffusion tensor imaging data: initial results. AJNR Am. J. Neuroradiol. 33, 2123–2128. https://doi.org/10.3174/ajnr.A3126

Haller, S., Lovblad, K.-O., Giannakopoulos, P., Van De Ville, D., 2014. Multivariate pattern recognition for diagnosis and prognosis in clinical neuroimaging: state of the art, current challenges and future trends. Brain Topogr. 27, 329–337. https://doi.org/10.1007/s10548-014-0360-z

Handwerker, D.A., Ollinger, J.M., D'Esposito, M., 2004. Variation of BOLD hemodynamic responses across subjects and brain regions and their effects on statistical analyses. NeuroImage 21, 1639–1651. https://doi.org/10.1016/j.neuroimage.2003.11.029

Henson, R.N.A., Price, C.J., Rugg, M.D., Turner, R., Friston, K.J., 2002. Detecting latency differences in event-related BOLD responses: application to words

versus nonwords and initial versus repeated face presentations. NeuroImage 15, 83–97. https://doi.org/10.1006/nimg.2001.0940
Ho, B.-C., Andreasen, N.C., Ziebell, S., Pierson, R., Magnotta, V., 2011. Long-term antipsychotic treatment and brain volumes: a longitudinal study of first-episode schizophrenia. Arch. Gen. Psychiatry 68, 128–137. https://doi.org/10.1001/archgenpsychiatry.2010.199
Hommes, J., Krabbendam, L., Versmissen, D., Kircher, T., van Os, J., van Winkel, R., 2012. Self-monitoring as a familial vulnerability marker for psychosis: an analysis of patients, unaffected siblings and healthy controls. Psychol. Med. 42, 235–245. https://doi.org/10.1017/S0033291711001152
Huber, G., Gross, G., 1989. The concept of basic symptoms in schizophrenic and schizoaffective psychoses. Recenti Prog. Med. 80, 646–652.
Iniesta, R., Stahl, D., McGuffin, P., 2016. Machine learning, statistical learning and the future of biological research in psychiatry. Psychol. Med. 46, 2455–2465. https://doi.org/10.1017/S0033291716001367
Iwabuchi, S.J., Liddle, P.F., Palaniyappan, L., 2015. Structural connectivity of the salience-executive loop in schizophrenia. Eur. Arch. Psychiatry Clin. Neurosci. 265, 163–166. https://doi.org/10.1007/s00406-014-0547-z
Jablensky, A., 2010. The diagnostic concept of schizophrenia: its history, evolution, and future prospects. Dialogues Clin. Neurosci. 12, 271–287.
Jardri, R., Pins, D., Lafargue, G., Very, E., Ameller, A., Delmaire, C., Thomas, P., 2011. Increased overlap between the brain areas involved in self-other distinction in schizophrenia. PloS One 6, e17500. https://doi.org/10.1371/journal.pone.0017500
Jeannerod, M., 2009. The sense of agency and its disturbances in schizophrenia: a reappraisal. Exp. Brain Res. 192, 527–532. https://doi.org/10.1007/s00221-008-1533-3
Jenkinson, M., Beckmann, C.F., Behrens, T.E.J., Woolrich, M.W., Smith, S.M., 2012. FSL. NeuroImage 62, 782–790. https://doi.org/10.1016/j.neuroimage.2011.09.015
Jenkinson, M., Smith, S., 2001. A global optimisation method for robust affine registration of brain images. Med. Image Anal. 5, 143–156.
Jones, D.K., Knösche, T.R., Turner, R., 2013. White matter integrity, fiber count, and other fallacies: The do's and don'ts of diffusion MRI. NeuroImage 73, 239–254. https://doi.org/10.1016/j.neuroimage.2012.06.081
Kambeitz, J., Kambeitz-Ilankovic, L., Leucht, S., Wood, S., Davatzikos, C., Malchow, B., Falkai, P., Koutsouleris, N., 2015a. Detecting neuroimaging biomarkers for schizophrenia: a meta-analysis of multivariate pattern recognition studies. Neuropsychopharmacol. Off. Publ. Am. Coll. Neuropsychopharmacol. 40, 1742–1751. https://doi.org/10.1038/npp.2015.22
Kambeitz, J., Kambeitz-Ilankovic, L., Leucht, S., Wood, S., Davatzikos, C., Malchow, B., Falkai, P., Koutsouleris, N., 2015b. Detecting neuroimaging biomarkers for schizophrenia: a meta-analysis of multivariate pattern recognition studies. Neuropsychopharmacol. Off. Publ. Am. Coll. Neuropsychopharmacol. 40, 1742–1751. https://doi.org/10.1038/npp.2015.22
Kasparek, T., Thomaz, C.E., Sato, J.R., Schwarz, D., Janousova, E., Marecek, R., Prikryl, R., Vanicek, J., Fujita, A., Ceskova, E., 2011. Maximum-uncertainty linear discrimination analysis of first-episode schizophrenia subjects. Psychiatry Res. 191, 174–181. https://doi.org/10.1016/j.pscychresns.2010.09.016

Kay, S.R., Fiszbein, A., Opler, L.A., 1987. The positive and negative syndrome scale (PANSS) for schizophrenia. Schizophr. Bull. 13, 261–276.

Kelly, S., Jahanshad, N., Zalesky, A., Kochunov, P., Agartz, I., Alloza, C., Andreassen, O.A., Arango, C., Banaj, N., Bouix, S., Bousman, C.A., Brouwer, R.M., Bruggemann, J., Bustillo, J., Cahn, W., Calhoun, V., Cannon, D., Carr, V., Catts, S., Chen, J., Chen, J.–., Chen, X., Chiapponi, C., Cho, K.K., Ciullo, V., Corvin, A.S., Crespo-Facorro, B., Cropley, V., De Rossi, P., Diaz-Caneja, C.M., Dickie, E.W., Ehrlich, S., Fan, F.–., Faskowitz, J., Fatouros-Bergman, H., Flyckt, L., Ford, J.M., Fouche, J.-P., Fukunaga, M., Gill, M., Glahn, D.C., Gollub, R., Goudzwaard, E.D., Guo, H., Gur, R.E., Gur, R.C., Gurholt, T.P., Hashimoto, R., Hatton, S.N., Henskens, F.A., Hibar, D.P., Hickie, I.B., Hong, L.E., Horacek, J., Howells, F.M., Hulshoff Pol, H.E., Hyde, C.L., Isaev, D., Jablensky, A., Jansen, P.R., Janssen, J., Jönsson, E.G., Jung, L.A., Kahn, R.S., Kikinis, Z., Liu, K., Klauser, P., Knöchel, C., Kubicki, M., Lagopoulos, J., Langen, C., Lawrie, S., Lenroot, R.K., Lim, K.O., Lopez-Jaramillo, C., Lyall, A., Magnotta, V., Mandl, R.C.W., Mathalon, D.H., McCarley, R.W., McCarthy-Jones, S., McDonald, C., McEwen, S., McIntosh, A., Melicher, T., Mesholam-Gately, R.I., Michie, P.T., Mowry, B., Mueller, B.A., Newell, D.T., O'Donnell, P., Oertel-Knöchel, V., Oestreich, L., Paciga, S.A., Pantelis, C., Pasternak, O., Pearlson, G., Pellicano, G.R., Pereira, A., Pineda Zapata, J., Piras, F., Potkin, S.G., Preda, A., Rasser, P.E., Roalf, D.R., Roiz, R., Roos, A., Rotenberg, D., Satterthwaite, T.D., Savadjiev, P., Schall, U., Scott, R.J., Seal, M.L., Seidman, L.J., Shannon Weickert, C., Whelan, C.D., Shenton, M.E., Kwon, J.S., Spalletta, G., Spaniel, F., Sprooten, E., Stäblein, M., Stein, D.J., Sundram, S., Tan, Y., Tan, S., Tang, S., Temmingh, H.S., Westlye, L.T., Tønnesen, S., Tordesillas-Gutierrez, D., Doan, N.T., Vaidya, J., van Haren, N.E.M., Vargas, C.D., Vecchio, D., Velakoulis, D., Voineskos, A., Voyvodic, J.Q., Wang, Z., Wan, P., Wei, D., Weickert, T.W., Whalley, H., White, T., Whitford, T.J., Wojcik, J.D., Xiang, H., Xie, Z., Yamamori, H., Yang, F., Yao, N., Zhang, G., Zhao, J., van Erp, T.G.M., Turner, J., Thompson, P.M., Donohoe, G., 2017. Widespread white matter microstructural differences in schizophrenia across 4322 individuals: results from the ENIGMA Schizophrenia DTI Working Group. Mol. Psychiatry. https://doi.org/10.1038/mp.2017.170

Kendell, R., Jablensky, A., 2003. Distinguishing Between the Validity and Utility of Psychiatric Diagnoses. Am. J. Psychiatry 160, 4–12. https://doi.org/10.1176/appi.ajp.160.1.4

Kolenic, M., Franke, K., Hlinka, J., Matejka, M., Capkova, J., Pausova, Z., Uher, R., Alda, M., Spaniel, F., Hajek, T., 2018. Obesity, dyslipidemia and brain age in first-episode psychosis. J. Psychiatr. Res. 99, 151–158. https://doi.org/10.1016/j.jpsychires.2018.02.012

Koutsouleris, N., Meisenzahl, E.M., Borgwardt, S., Riecher-Rössler, A., Frodl, T., Kambeitz, J., Köhler, Y., Falkai, P., Möller, H.-J., Reiser, M., Davatzikos, C., 2015. Individualized differential diagnosis of schizophrenia and mood disorders using neuroanatomical biomarkers. Brain J. Neurol. https://doi.org/10.1093/brain/awv111

Koutsouleris, N., Wobrock, T., Guse, B., Langguth, B., Landgrebe, M., Eichhammer, P., Frank, E., Cordes, J., Wölwer, W., Musso, F., Winterer, G., Gaebel, W., Hajak, G., Ohmann, C., Verde, P.E., Rietschel, M., Ahmed, R., Honer, W.G., Dwyer, D., Ghaseminejad, F., Dechent, P., Malchow, B., Kreuzer, P.M., Poeppl, T.B., Schneider-Axmann, T., Falkai, P., Hasan, A., 2017. Predicting Response to

Repetitive Transcranial Magnetic Stimulation in Patients With Schizophrenia Using Structural Magnetic Resonance Imaging: A Multisite Machine Learning Analysis. Schizophr. Bull. https://doi.org/10.1093/schbul/sbx114
LaConte, S., Strother, S., Cherkassky, V., Anderson, J., Hu, X., 2005a. Support vector machines for temporal classification of block design fMRI data. NeuroImage 26, 317–329. https://doi.org/10.1016/j.neuroimage.2005.01.048
LaConte, S., Strother, S., Cherkassky, V., Anderson, J., Hu, X., 2005b. Support vector machines for temporal classification of block design fMRI data. NeuroImage 26, 317–329. https://doi.org/10.1016/j.neuroimage.2005.01.048
Lamers, F., Milaneschi, Y., de Jonge, P., Giltay, E.J., Penninx, B.W.J.H., 2017. Metabolic and inflammatory markers: associations with individual depressive symptoms. Psychol. Med. 1–11. https://doi.org/10.1017/S0033291717002483
Lancaster, J.L., Woldorff, M.G., Parsons, L.M., Liotti, M., Freitas, C.S., Rainey, L., Kochunov, P.V., Nickerson, D., Mikiten, S.A., Fox, P.T., 2000. Automated Talairach atlas labels for functional brain mapping. Hum. Brain Mapp. 10, 120–131.
Lecrubier, Y., Sheehan, D.V., Weiller, E., Amorim, P., Bonora, I., Harnett Sheehan, K., Janavs, J., Dunbar, G.C., 1997. The Mini International Neuropsychiatric Interview (MINI). A short diagnostic structured interview: reliability and validity according to the CIDI. Eur. Psychiatry 12, 224–231. https://doi.org/10.1016/S0924-9338(97)83296-8
Levav, I., Rutz, W., 2002. The WHO World Health Report 2001 new understanding--new hope. Isr. J. Psychiatry Relat. Sci. 39, 50–56.
Lieberman, J., Chakos, M., Wu, H., Alvir, J., Hoffman, E., Robinson, D., Bilder, R., 2001. Longitudinal study of brain morphology in first episode schizophrenia. Biol. Psychiatry 49, 487–499.
Malla, A.K., Bodnar, M., Joober, R., Lepage, M., 2011. Duration of untreated psychosis is associated with orbital–frontal grey matter volume reductions in first episode psychosis. Schizophr. Res. 125, 13–20. https://doi.org/10.1016/j.schres.2010.09.021
Malonek, D., Grinvald, A., 1996. Interactions between electrical activity and cortical microcirculation revealed by imaging spectroscopy: implications for functional brain mapping. Science 272, 551–554.
Manoliu, A., Riedl, V., Zherdin, A., Muhlau, M., Schwerthoffer, D., Scherr, M., Peters, H., Zimmer, C., Forstl, H., Bauml, J., Wohlschlager, A.M., Sorg, C., 2014. Aberrant Dependence of Default Mode/Central Executive Network Interactions on Anterior Insular Salience Network Activity in Schizophrenia. Schizophr. Bull. 40, 428–437. https://doi.org/10.1093/schbul/sbt037
Melicher, T., Horacek, J., Hlinka, J., Spaniel, F., Tintera, J., Ibrahim, I., Mikolas, P., Novak, T., Mohr, P., Hoschl, C., 2015a. White matter changes in first episode psychosis and their relation to the size of sample studied: a DTI study. Schizophr. Res. 162, 22–28. https://doi.org/10.1016/j.schres.2015.01.029
Melicher, T., Horacek, J., Hlinka, J., Spaniel, F., Tintera, J., Ibrahim, I., Mikolas, P., Novak, T., Mohr, P., Hoschl, C., 2015b. White matter changes in first episode psychosis and their relation to the size of sample studied: a DTI study. Schizophr. Res. 162, 22–28. https://doi.org/10.1016/j.schres.2015.01.029
Menon, V., Uddin, L.Q., 2010a. Saliency, switching, attention and control: a network model of insula function. Brain Struct. Funct. 214, 655–667. https://doi.org/10.1007/s00429-010-0262-0

Menon, V., Uddin, L.Q., 2010b. Saliency, switching, attention and control: a network model of insula function. Brain Struct. Funct. 214, 655–667. https://doi.org/10.1007/s00429-010-0262-0

Mikolas, P., Hlinka, J., Skoch, A., Pitra, Z., Frodl, T., Spaniel, F., Hajek, T., 2018. Machine learning classification of first-episode schizophrenia spectrum disorders and controls using whole brain white matter fractional anisotropy. BMC Psychiatry 18. https://doi.org/10.1186/s12888-018-1678-y

Mikolas, P., Melicher, T., Skoch, A., Matejka, M., Slovakova, A., Bakstein, E., Hajek, T., Spaniel, F., 2016. Connectivity of the anterior insula differentiates participants with first-episode schizophrenia spectrum disorders from controls: a machine-learning study. Psychol. Med. 46, 2695–2704. https://doi.org/10.1017/S0033291716000878

Milham, M.P., Craddock, R.C., Klein, A., 2017a. Clinically useful brain imaging for neuropsychiatry: How can we get there? Depress. Anxiety 34, 578–587. https://doi.org/10.1002/da.22627

Milham, M.P., Craddock, R.C., Klein, A., 2017b. Clinically useful brain imaging for neuropsychiatry: How can we get there? Depress. Anxiety 34, 578–587. https://doi.org/10.1002/da.22627

Mourao-Miranda, J., Reinders, A. a. T.S., Rocha-Rego, V., Lappin, J., Rondina, J., Morgan, C., Morgan, K.D., Fearon, P., Jones, P.B., Doody, G.A., Murray, R.M., Kapur, S., Dazzan, P., 2012a. Individualized prediction of illness course at the first psychotic episode: a support vector machine MRI study. Psychol. Med. 42, 1037–1047. https://doi.org/10.1017/S0033291711002005

Mourao-Miranda, J., Reinders, A. a. T.S., Rocha-Rego, V., Lappin, J., Rondina, J., Morgan, C., Morgan, K.D., Fearon, P., Jones, P.B., Doody, G.A., Murray, R.M., Kapur, S., Dazzan, P., 2012b. Individualized prediction of illness course at the first psychotic episode: a support vector machine MRI study. Psychol. Med. 42, 1037–1047. https://doi.org/10.1017/S0033291711002005

Mourao-Miranda, J., Reinders, A. a. T.S., Rocha-Rego, V., Lappin, J., Rondina, J., Morgan, C., Morgan, K.D., Fearon, P., Jones, P.B., Doody, G.A., Murray, R.M., Kapur, S., Dazzan, P., 2012c. Individualized prediction of illness course at the first psychotic episode: a support vector machine MRI study. Psychol. Med. 42, 1037–1047. https://doi.org/10.1017/S0033291711002005

Moussa, M.N., Steen, M.R., Laurienti, P.J., Hayasaka, S., 2012. Consistency of Network Modules in Resting-State fMRI Connectome Data. PLOS ONE 7, e44428. https://doi.org/10.1371/journal.pone.0044428

Murray, R.J., Schaer, M., Debbané, M., 2012. Degrees of separation: a quantitative neuroimaging meta-analysis investigating self-specificity and shared neural activation between self- and other-reflection. Neurosci. Biobehav. Rev. 36, 1043–1059. https://doi.org/10.1016/j.neubiorev.2011.12.013

Mwansisya, T.E., Hu, A., Li, Y., Chen, X., Wu, G., Huang, X., Lv, D., Li, Z., Liu, C., Xue, Z., Feng, J., Liu, Z., 2017. Task and resting-state fMRI studies in first-episode schizophrenia: A systematic review. Schizophr. Res. https://doi.org/10.1016/j.schres.2017.02.026

Nekovarova, T., Fajnerova, I., Horacek, J., Spaniel, F., 2014. Bridging disparate symptoms of schizophrenia: a triple network dysfunction theory. Front. Behav. Neurosci. 8, 171. https://doi.org/10.3389/fnbeh.2014.00171

Nichols, T.E., Holmes, A.P., 2002. Nonparametric permutation tests for functional neuroimaging: a primer with examples. Hum. Brain Mapp. 15, 1–25.

Nieuwenhuis, M., van Haren, N.E.M., Hulshoff Pol, H.E., Cahn, W., Kahn, R.S., Schnack, H.G., 2012. Classification of schizophrenia patients and healthy controls from structural MRI scans in two large independent samples. NeuroImage 61, 606–612. https://doi.org/10.1016/j.neuroimage.2012.03.079

Nilsson, R., Björkegren, J., Tegner, J., 2006. A Flexible Implementation for Support Vector Machines.

Northoff, G., Heinzel, A., de Greck, M., Bermpohl, F., Dobrowolny, H., Panksepp, J., 2006. Self-referential processing in our brain--a meta-analysis of imaging studies on the self. NeuroImage 31, 440–457. https://doi.org/10.1016/j.neuroimage.2005.12.002

Obhi, S.S., Hall, P., 2011. Sense of agency in joint action: influence of human and computer co-actors. Exp. Brain Res. 211, 663–670. https://doi.org/10.1007/s00221-011-2662-7

Ogawa, S., Menon, R.S., Tank, D.W., Kim, S.G., Merkle, H., Ellermann, J.M., Ugurbil, K., 1993. Functional brain mapping by blood oxygenation level-dependent contrast magnetic resonance imaging. A comparison of signal characteristics with a biophysical model. Biophys. J. 64, 803–812.

Palaniyappan, L., Simmonite, M., White, T.P., Liddle, E.B., Liddle, P.F., 2013a. Neural primacy of the salience processing system in schizophrenia. Neuron 79, 814–828. https://doi.org/10.1016/j.neuron.2013.06.027

Palaniyappan, L., Simmonite, M., White, T.P., Liddle, E.B., Liddle, P.F., 2013b. Neural primacy of the salience processing system in schizophrenia. Neuron 79, 814–828. https://doi.org/10.1016/j.neuron.2013.06.027

Penttilä, M., Jääskeläinen, E., Haapea, M., Tanskanen, P., Veijola, J., Ridler, K., Murray, G.K., Barnes, A., Jones, P.B., Isohanni, M., Koponen, H., Miettunen, J., 2010. Association between duration of untreated psychosis and brain morphology in schizophrenia within the Northern Finland 1966 Birth Cohort. Schizophr. Res. 123, 145–152. https://doi.org/10.1016/j.schres.2010.08.016

Pereira, F., Mitchell, T., Botvinick, M., 2009a. Machine learning classifiers and fMRI: A tutorial overview. NeuroImage 45, S199–S209. https://doi.org/10.1016/j.neuroimage.2008.11.007

Pereira, F., Mitchell, T., Botvinick, M., 2009b. Machine learning classifiers and fMRI: A tutorial overview. NeuroImage 45, S199–S209. https://doi.org/10.1016/j.neuroimage.2008.11.007

Perkins, D.O., Gu, H., Boteva, K., Lieberman, J.A., 2005. Relationship Between Duration of Untreated Psychosis and Outcome in First-Episode Schizophrenia: A Critical Review and Meta-Analysis. Am. J. Psychiatry 162, 1785–1804. https://doi.org/10.1176/appi.ajp.162.10.1785

Peruzzo, D., Castellani, U., Perlini, C., Bellani, M., Marinelli, V., Rambaldelli, G., Lasalvia, A., Tosato, S., De Santi, K., Murino, V., Ruggeri, M., Brambilla, P., PICOS-Veneto Group, 2014. Classification of first-episode psychosis: a multi-modal multi-feature approach integrating structural and diffusion imaging. J. Neural Transm. Vienna Austria 1996. https://doi.org/10.1007/s00702-014-1324-x

Pettersson-Yeo, W., Benetti, S., Marquand, A.F., Dell'acqua, F., Williams, S.C.R., Allen, P., Prata, D., McGuire, P., Mechelli, A., 2013a. Using genetic, cognitive and multi-modal neuroimaging data to identify ultra-high-risk and first-episode psychosis at the individual level. Psychol. Med. 43, 2547–2562. https://doi.org/10.1017/S003329171300024X

Pettersson-Yeo, W., Benetti, S., Marquand, A.F., Dell'acqua, F., Williams, S.C.R., Allen, P., Prata, D., McGuire, P., Mechelli, A., 2013b. Using genetic, cognitive and multi-modal neuroimaging data to identify ultra-high-risk and first-episode psychosis at the individual level. Psychol. Med. 43, 2547–2562. https://doi.org/10.1017/S003329171300024X

Pettersson-Yeo, W., Benetti, S., Marquand, A.F., Dell'acqua, F., Williams, S.C.R., Allen, P., Prata, D., McGuire, P., Mechelli, A., 2013c. Using genetic, cognitive and multi-modal neuroimaging data to identify ultra-high-risk and first-episode psychosis at the individual level. Psychol. Med. 43, 2547–2562. https://doi.org/10.1017/S003329171300024X

Preti, A., Cella, M., 2010. Randomized-controlled trials in people at ultra high risk of psychosis: a review of treatment effectiveness. Schizophr. Res. 123, 30–36. https://doi.org/10.1016/j.schres.2010.07.026

Propper, L., Ortiz, A., Slaney, C., Garnham, J., Ruzickova, M., Calkin, C.V., O'Donovan, C., Hajek, T., Alda, M., 2015. Early-onset and very-early-onset bipolar disorder: distinct or similar clinical conditions? Bipolar Disord. 17, 814–820. https://doi.org/10.1111/bdi.12346

Rabinowitz, J., Levine, S.Z., Haim, R., Häfner, H., 2007. The course of schizophrenia: progressive deterioration, amelioration or both? Schizophr. Res. 91, 254–258. https://doi.org/10.1016/j.schres.2006.12.013

Rao, A., Monteiro, J.M., Mourao-Miranda, J., 2017. Predictive modelling using neuroimaging data in the presence of confounds. NeuroImage 150, 23–49. https://doi.org/10.1016/j.neuroimage.2017.01.066

Rasmussen, C.E., Williams, C.K.I., 2008. Gaussian processes for machine learning, 3. print. ed, Adaptive computation and machine learning. MIT Press, Cambridge, Mass.

Ren, W., Lui, S., Deng, W., Li, F., Li, M., Huang, X., Wang, Y., Li, T., Sweeney, J.A., Gong, Q., 2013. Anatomical and Functional Brain Abnormalities in Drug-Naive First-Episode Schizophrenia. Am. J. Psychiatry 170, 1308–1316. https://doi.org/10.1176/appi.ajp.2013.12091148

Rocha-Rego, V., Jogia, J., Marquand, A.F., Mourao-Miranda, J., Simmons, A., Frangou, S., 2014. Examination of the predictive value of structural magnetic resonance scans in bipolar disorder: a pattern classification approach. Psychol. Med. 44, 519–532. https://doi.org/10.1017/S0033291713001013

Samartzis, L., Dima, D., Fusar-Poli, P., Kyriakopoulos, M., 2014. White Matter Alterations in Early Stages of Schizophrenia: A Systematic Review of Diffusion Tensor Imaging Studies. J. Neuroimaging 24, 101–110. https://doi.org/10.1111/j.1552-6569.2012.00779.x

Sarpal, D.K., Robinson, D.G., Lencz, T., Argyelan, M., Ikuta, T., Karlsgodt, K., Gallego, J.A., Kane, J.M., Szeszko, P.R., Malhotra, A.K., 2015. Antipsychotic treatment and functional connectivity of the striatum in first-episode schizophrenia. JAMA Psychiatry 72, 5–13. https://doi.org/10.1001/jamapsychiatry.2014.1734

Schnack, H.G., Nieuwenhuis, M., van Haren, N.E.M., Abramovic, L., Scheewe, T.W., Brouwer, R.M., Hulshoff Pol, H.E., Kahn, R.S., 2014. Can structural MRI aid in clinical classification? A machine learning study in two independent samples of patients with schizophrenia, bipolar disorder and healthy subjects. NeuroImage 84, 299–306. https://doi.org/10.1016/j.neuroimage.2013.08.053

Schnack, H.G., van Haren, N.E.M., Brouwer, R.M., van Baal, G.C.M., Picchioni, M., Weisbrod, M., Sauer, H., Cannon, T.D., Huttunen, M., Lepage, C., Collins, D.L., Evans, A., Murray, R.M., Kahn, R.S., Hulshoff Pol, H.E., 2010. Mapping

reliability in multicenter MRI: Voxel-based morphometry and cortical thickness. Hum. Brain Mapp. 31, 1967–1982. https://doi.org/10.1002/hbm.20991
Schnack, H.G., van Haren, N.E.M., Nieuwenhuis, M., Hulshoff Pol, H.E., Cahn, W., Kahn, R.S., 2016. Accelerated Brain Aging in Schizophrenia: A Longitudinal Pattern Recognition Study. Am. J. Psychiatry 173, 607–616. https://doi.org/10.1176/appi.ajp.2015.15070922
Schrouff, J., Rosa, M.J., Rondina, J.M., Marquand, A.F., Chu, C., Ashburner, J., Phillips, C., Richiardi, J., Mourão-Miranda, J., 2013. PRoNTo: pattern recognition for neuroimaging toolbox. Neuroinformatics 11, 319–337. https://doi.org/10.1007/s12021-013-9178-1
Schultze-Lutter, F., 2009. Subjective Symptoms of Schizophrenia in Research and the Clinic: The Basic Symptom Concept. Schizophr. Bull. 35, 5–8. https://doi.org/10.1093/schbul/sbn139
Shawe-Taylor, J., Cristianini, N., 2006. Kernel methods for pattern analysis, 3rd printing. ed. Cambridge University Press, Cambridge.
Smieskova, R., Fusar-Poli, P., Allen, P., Bendfeldt, K., Stieglitz, R.D., Drewe, J., Radue, E.W., McGuire, P.K., Riecher-Rössler, A., Borgwardt, S.J., 2009. The effects of antipsychotics on the brain: what have we learnt from structural imaging of schizophrenia?--a systematic review. Curr. Pharm. Des. 15, 2535–2549.
Smith, S.M., Jenkinson, M., Johansen-Berg, H., Rueckert, D., Nichols, T.E., Mackay, C.E., Watkins, K.E., Ciccarelli, O., Cader, M.Z., Matthews, P.M., Behrens, T.E.J., 2006. Tract-based spatial statistics: voxelwise analysis of multi-subject diffusion data. NeuroImage 31, 1487–1505. https://doi.org/10.1016/j.neuroimage.2006.02.024
Smith, S.M., Jenkinson, M., Woolrich, M.W., Beckmann, C.F., Behrens, T.E.J., Johansen-Berg, H., Bannister, P.R., De Luca, M., Drobnjak, I., Flitney, D.E., Niazy, R.K., Saunders, J., Vickers, J., Zhang, Y., De Stefano, N., Brady, J.M., Matthews, P.M., 2004. Advances in functional and structural MR image analysis and implementation as FSL. NeuroImage 23 Suppl 1, S208-219. https://doi.org/10.1016/j.neuroimage.2004.07.051
Song, X.-W., Dong, Z.-Y., Long, X.-Y., Li, S.-F., Zuo, X.-N., Zhu, C.-Z., He, Y., Yan, C.-G., Zang, Y.-F., 2011. REST: a toolkit for resting-state functional magnetic resonance imaging data processing. PloS One 6, e25031. https://doi.org/10.1371/journal.pone.0025031
Spaniel, F., Tintera, J., Rydlo, J., Ibrahim, I., Kasparek, T., Horacek, J., Zaytseva, Y., Matejka, M., Fialova, M., Slovakova, A., Mikolas, P., Melicher, T., Görnerova, N., Höschl, C., Hajek, T., 2016. Altered Neural Correlate of the Self-Agency Experience in First-Episode Schizophrenia-Spectrum Patients: An fMRI Study. Schizophr. Bull. 42, 916–925. https://doi.org/10.1093/schbul/sbv188
Sperduti, M., Delaveau, P., Fossati, P., Nadel, J., 2011. Different brain structures related to self- and external-agency attribution: a brief review and meta-analysis. Brain Struct. Funct. 216, 151–157. https://doi.org/10.1007/s00429-010-0298-1
Sridharan, D., Levitin, D.J., Menon, V., 2008. A critical role for the right fronto-insular cortex in switching between central-executive and default-mode networks. Proc. Natl. Acad. Sci. U. S. A. 105, 12569–12574. https://doi.org/10.1073/pnas.0800005105
Sundermann, B., Herr, D., Schwindt, W., Pfleiderer, B., 2014. Multivariate classification of blood oxygen level-dependent FMRI data with diagnostic intention: a clinical perspective. AJNR Am. J. Neuroradiol. 35, 848–855. https://doi.org/10.3174/ajnr.A3713

Swanson, N., Eichele, T., Pearlson, G., Kiehl, K., Yu, Q., Calhoun, V.D., 2011. Lateral Differences in the Default Mode Network in Healthy Controls and Schizophrenia Patients. Hum. Brain Mapp. 32, 654–664. https://doi.org/10.1002/hbm.21055

Takahashi, T., Wood, S.J., Yung, A.R., Phillips, L.J., Soulsby, B., McGorry, P.D., Tanino, R., Zhou, S.-Y., Suzuki, M., Velakoulis, D., al, et, 2009. Insular cortex gray matter changes in individuals at ultra-high-risk of developing psychosis. Schizophr. Res. 111, 94–102. https://doi.org/10.1016/j.schres.2009.03.024

the Alzheimer's Disease Neuroimaging Initiative, EPIGEN Consortium, IMAGEN Consortium, Saguenay Youth Study (SYS) Group, Thompson, P.M., Stein, J.L., Medland, S.E., Hibar, D.P., Vasquez, A.A., Renteria, M.E., Toro, R., Jahanshad, N., Schumann, G., Franke, B., Wright, M.J., Martin, N.G., Agartz, I., Alda, M., Alhusaini, S., Almasy, L., Almeida, J., Alpert, K., Andreasen, N.C., Andreassen, O.A., Apostolova, L.G., Appel, K., Armstrong, N.J., Aribisala, B., Bastin, M.E., Bauer, M., Bearden, C.E., Bergmann, Ø., Binder, E.B., Blangero, J., Bockholt, H.J., Bøen, E., Bois, C., Boomsma, D.I., Booth, T., Bowman, I.J., Bralten, J., Brouwer, R.M., Brunner, H.G., Brohawn, D.G., Buckner, R.L., Buitelaar, J., Bulayeva, K., Bustillo, J.R., Calhoun, V.D., Cannon, D.M., Cantor, R.M., Carless, M.A., Caseras, X., Cavalleri, G.L., Chakravarty, M.M., Chang, K.D., Ching, C.R.K., Christoforou, A., Cichon, S., Clark, V.P., Conrod, P., Coppola, G., Crespo-Facorro, B., Curran, J.E., Czisch, M., Deary, I.J., de Geus, E.J.C., den Braber, A., Delvecchio, G., Depondt, C., de Haan, L., de Zubicaray, G.I., Dima, D., Dimitrova, R., Djurovic, S., Dong, H., Donohoe, G., Duggirala, R., Dyer, T.D., Ehrlich, S., Ekman, C.J., Elvsåshagen, T., Emsell, L., Erk, S., Espeseth, T., Fagerness, J., Fears, S., Fedko, I., Fernández, G., Fisher, S.E., Foroud, T., Fox, P.T., Francks, C., Frangou, S., Frey, E.M., Frodl, T., Frouin, V., Garavan, H., Giddaluru, S., Glahn, D.C., Godlewska, B., Goldstein, R.Z., Gollub, R.L., Grabe, H.J., Grimm, O., Gruber, O., Guadalupe, T., Gur, R.E., Gur, R.C., Göring, H.H.H., Hagenaars, S., Hajek, T., Hall, G.B., Hall, J., Hardy, J., Hartman, C.A., Hass, J., Hatton, S.N., Haukvik, U.K., Hegenscheid, K., Heinz, A., Hickie, I.B., Ho, B.-C., Hoehn, D., Hoekstra, P.J., Hollinshead, M., Holmes, A.J., Homuth, G., Hoogman, M., Hong, L.E., Hosten, N., Hottenga, J.-J., Hulshoff Pol, H.E., Hwang, K.S., Jack, C.R., Jenkinson, M., Johnston, C., Jönsson, E.G., Kahn, R.S., Kasperaviciute, D., Kelly, S., Kim, S., Kochunov, P., Koenders, L., Krämer, B., Kwok, J.B.J., Lagopoulos, J., Laje, G., Landen, M., Landman, B.A., Lauriello, J., Lawrie, S.M., Lee, P.H., Le Hellard, S., Lemaître, H., Leonardo, C.D., Li, C., Liberg, B., Liewald, D.C., Liu, X., Lopez, L.M., Loth, E., Lourdusamy, A., Luciano, M., Macciardi, F., Machielsen, M.W.J., MacQueen, G.M., Malt, U.F., Mandl, R., Manoach, D.S., Martinot, J.-L., Matarin, M., Mather, K.A., Mattheisen, M., Mattingsdal, M., Meyer-Lindenberg, A., McDonald, C., McIntosh, A.M., McMahon, F.J., McMahon, K.L., Meisenzahl, E., Melle, I., Milaneschi, Y., Mohnke, S., Montgomery, G.W., Morris, D.W., Moses, E.K., Mueller, B.A., Muñoz Maniega, S., Mühleisen, T.W., Müller-Myhsok, B., Mwangi, B., Nauck, M., Nho, K., Nichols, T.E., Nilsson, L.-G., Nugent, A.C., Nyberg, L., Olvera, R.L., Oosterlaan, J., Ophoff, R.A., Pandolfo, M., Papalampropoulou-Tsiridou, M., Papmeyer, M., Paus, T., Pausova, Z., Pearlson, G.D., Penninx, B.W., Peterson, C.P., Pfennig, A., Phillips, M., Pike, G.B., Poline, J.-B., Potkin, S.G., Pütz, B., Ramasamy, A., Rasmussen, J., Rietschel, M., Rijpkema, M., Risacher, S.L., Roffman, J.L., Roiz-Santiañez, R., Romanczuk-Seiferth, N., Rose, E.J., Royle, N.A., Rujescu, D., Ryten, M.,

Sachdev, P.S., Salami, A., Satterthwaite, T.D., Savitz, J., Saykin, A.J., Scanlon, C., Schmaal, L., Schnack, H.G., Schork, A.J., Schulz, S.C., Schür, R., Seidman, L., Shen, L., Shoemaker, J.M., Simmons, A., Sisodiya, S.M., Smith, C., Smoller, J.W., Soares, J.C., Sponheim, S.R., Sprooten, E., Starr, J.M., Steen, V.M., Strakowski, S., Strike, L., Sussmann, J., Sämann, P.G., Teumer, A., Toga, A.W., Tordesillas-Gutierrez, D., Trabzuni, D., Trost, S., Turner, J., Van den Heuvel, M., van der Wee, N.J., van Eijk, K., van Erp, T.G.M., van Haren, N.E.M., van 't Ent, D., van Tol, M.-J., Valdés Hernández, M.C., Veltman, D.J., Versace, A., Völzke, H., Walker, R., Walter, H., Wang, L., Wardlaw, J.M., Weale, M.E., Weiner, M.W., Wen, W., Westlye, L.T., Whalley, H.C., Whelan, C.D., White, T., Winkler, A.M., Wittfeld, K., Woldehawariat, G., Wolf, C., Zilles, D., Zwiers, M.P., Thalamuthu, A., Schofield, P.R., Freimer, N.B., Lawrence, N.S., Drevets, W., 2014. The ENIGMA Consortium: large-scale collaborative analyses of neuroimaging and genetic data. Brain Imaging Behav. https://doi.org/10.1007/s11682-013-9269-5

Tzourio-Mazoyer, N., Landeau, B., Papathanassiou, D., Crivello, F., Etard, O., Delcroix, N., Mazoyer, B., Joliot, M., 2002. Automated anatomical labeling of activations in SPM using a macroscopic anatomical parcellation of the MNI MRI single-subject brain. NeuroImage 15, 273–289. https://doi.org/10.1006/nimg.2001.0978

Varoquaux, G., Craddock, R.C., 2013. Learning and comparing functional connectomes across subjects. NeuroImage 80, 405–415. https://doi.org/10.1016/j.neuroimage.2013.04.007

Venkataraman, A., Whitford, T.J., Westin, C.-F., Golland, P., Kubicki, M., 2012. Whole brain resting state functional connectivity abnormalities in schizophrenia. Schizophr. Res. 139, 7–12. https://doi.org/10.1016/j.schres.2012.04.021

Vita, A., De Peri, L., Deste, G., Sacchetti, E., 2012. Progressive loss of cortical gray matter in schizophrenia: a meta-analysis and meta-regression of longitudinal MRI studies. Transl. Psychiatry 2, e190. https://doi.org/10.1038/tp.2012.116

Voineskos, A.N., Foussias, G., Lerch, J., Felsky, D., Remington, G., Rajji, T.K., Lobaugh, N., Pollock, B.G., Mulsant, B.H., 2013. Neuroimaging evidence for the deficit subtype of schizophrenia. JAMA Psychiatry 70, 472–480. https://doi.org/10.1001/jamapsychiatry.2013.786

Whelan, R., Garavan, H., 2014. When optimism hurts: inflated predictions in psychiatric neuroimaging. Biol. Psychiatry 75, 746–748. https://doi.org/10.1016/j.biopsych.2013.05.014

White, T.P., Joseph, V., Francis, S.T., Liddle, P.F., 2010. Aberrant salience network (bilateral insula and anterior cingulate cortex) connectivity during information processing in schizophrenia. Schizophr. Res. 123, 105–115. https://doi.org/10.1016/j.schres.2010.07.020

Winkler, A.M., Ridgway, G.R., Webster, M.A., Smith, S.M., Nichols, T.E., 2014. Permutation inference for the general linear model. NeuroImage 92, 381–397. https://doi.org/10.1016/j.neuroimage.2014.01.060

Wu, M.-J., Mwangi, B., Bauer, I.E., Passos, I.C., Sanches, M., Zunta-Soares, G.B., Meyer, T.D., Hasan, K.M., Soares, J.C., 2016. Identification and individualized prediction of clinical phenotypes in bipolar disorders using neurocognitive data, neuroimaging scans and machine learning. NeuroImage. https://doi.org/10.1016/j.neuroimage.2016.02.016

Yao, L., Lui, S., Liao, Y., Du, M.-Y., Hu, N., Thomas, J.A., Gong, Q.-Y., 2013. White matter deficits in first episode schizophrenia: An activation likelihood estimation meta-analysis. Prog. Neuropsychopharmacol. Biol. Psychiatry 45, 100–106. https://doi.org/10.1016/j.pnpbp.2013.04.019

Zanetti, M.V., Schaufelberger, M.S., Doshi, J., Ou, Y., Ferreira, L.K., Menezes, P.R., Scazufca, M., Davatzikos, C., Busatto, G.F., 2013a. Neuroanatomical pattern classification in a population-based sample of first-episode schizophrenia. Prog. Neuropsychopharmacol. Biol. Psychiatry 43, 116–125. https://doi.org/10.1016/j.pnpbp.2012.12.005

Zanetti, M.V., Schaufelberger, M.S., Doshi, J., Ou, Y., Ferreira, L.K., Menezes, P.R., Scazufca, M., Davatzikos, C., Busatto, G.F., 2013b. Neuroanatomical pattern classification in a population-based sample of first-episode schizophrenia. Prog. Neuropsychopharmacol. Biol. Psychiatry 43, 116–125. https://doi.org/10.1016/j.pnpbp.2012.12.005